

**Double-Strand Breaks (DSBs) and Structure
Transition on Genome-sized DNA**

by

Ma Yue

Doshisha University

Graduate School of Life and Medical Sciences

May 2018

Doshisha University

Faculty of Life and Medical Sciences

Abstract

Double-Strand Breaks (DSBs) and Structure Transition on Genome-sized DNA

by Ma Yue

SUPERVISOR: Professor Kenichi Yoshikawa

The protective effect of ascorbic acid (AA) and DMSO against double-strand breaks (DSBs) in DNA was evaluated by single-molecule observation of giant DNA (T4 DNA; 166kbp) through fluorescence microscopy. Samples were exposed to three different forms of radiation: visible light, γ -ray, and ultrasound or freeze/thawing.

Ascorbic acid, or vitamin C, is a representative antioxidant. With regard to irradiation with visible light, 1 mM AA reduced the damage down to ca.30%. Same concentration of AA decreased the damage done by γ -ray to ca.70%. However, AA had almost no protective effect against the damage caused by ultrasound. This significant difference is discussed in relation to the physico-chemical mechanism of double-strand breaks depending on the radiation source.

Dimethyl sulphoxide (DMSO) is widely used as a cryoprotectant for organs, tissues, and cell suspension in storage. To date, many *in vitro* assays using cultured cells have been performed for analysing the protective effect of DMSO against genomic DNA damage; however, there have been few reports on the direct and

quantitative detection of DNA double strand breaks (DSBs) using single-molecule observation.

For the result of DMSO's protection on DSBs, we found that 2% DMSO conferred the maximum protective effect against all of the injury sources tested, and these effects were maintained at higher concentrations. Further, DMSO showed a significantly higher protective effect against freezing-induced damage than against photo- and γ -ray-irradiation-induced damage. Thus, the current data revealed that DMSO exhibits a protective effect in a dose dependent manner. Our study provides significant data for the optimization of DNA cryopreservation.

The change of the higher-order structure of genomic DNA molecules in the presence of alcohols by use of single DNA observation with fluorescence microscopy, by focusing our attention to unveil the different effect between 1-propanol and 2-propanol. We found that, with 1-propanol, the long-axis length exhibits minimum at 60% and then tends to increase with the increase of alcohol content. On the other hand, with 2-propanol the long-axis length exhibits almost monotonous decrease with the increase of alcohol content. These results indicate that DNA undergoes reentrant transition of coil-globule-coil with 1-propanol, whereas such reentrance phenomenon does not appear with 2-propanol.

Table of Contents

Abstract.....	i
Table of Contents	iii
List of Figures.....	vi
Acknowledgements	x
Chapter 1 General Introduction	1
1.1 Research history of DNA	1
1.2 Basic structure of DNA.....	2
1.3 Double-strand breaks (DSBs) of DNA.....	2
1.4 High-order structure transition of DNA	3
1.5 Secondary structure of DNA.....	4
1.6 Organizations of thesis.....	4
Chapter 2 Protective Effect of Ascorbic Acid against Double-strand Breaks in Giant DNA: Marked Differences among the Damage Induced by Photo-irradiation, Gamma-rays and Ultrasound	6
2.1 Introduction.....	6
2.2 Materials and Methods.....	7
2.2.1 Materials.....	7
2.2.2 Real-time observation of photo-induced breakage.....	7
2.2.3 Gamma-ray and ultrasound irradiation	8
2.2.4 Measurement of the length of single DNA molecules by fluorescence microscopy	9

2.3. Results and Analysis	9
2.3.1 Protective effect of ascorbic acid against photo-induced DNA double-strand breaks	9
2.3.2 Protective effect of ascorbic acid against gamma-ray-induced DNA double-strand breaks	12
2.3.3 Protective effect of ascorbic acid against ultrasound-induced DNA double-strand breaks	13
2.3.4 Comparison of the protective effects of ascorbic acid among photo-irradiation, gamma-rays and ultrasound	14
2.4. Discussion	15
Chapter 3 Protective Effect of DMSO against Double-strand Breaks in Giant DNA: Differences among the Damage induced by Photo-and γ-ray-irradiation, and Freezing	17
3.1 Introduction.....	17
3.2 Materials and Methods.....	19
3.2.1 Materials.....	19
3.2.2 Real-time observation of photo-induced breakage.....	19
3.2.3 Measurements of the contour length of DNA molecules to evaluate the injury caused by γ -ray and freezing.....	20
3.3 Results.....	21
3.3.1 Protective effect of DMSO against DSBs caused by photo-irradiation-induced ROS	21

3.3.2 Protective effect of DMSO against γ -ray-induced DSBs	23
3.3.4 Protective effect of DMSO against freezing-induced DSBs	25
3.4 Discussion	26
Chapter 4 Specific structural changes of DNA molecule in various alcohol solutions	28
4.1 Introduction	28
4.2 Materials and Methods	30
4.2.1 Materials	30
4.2.2 Single molecule observation of DNA through fluorescence microscope	30
4.2.3 Measurement of DNA secondary structure through circular dichroism (CD) spectra	31
4.3 Results	31
4.3.1 High-order structure of DNA molecules in propanols solutions	31
Chapter 5 General Conclusion.....	36
5.1 The protective effects of ascorbic acid against double-strand breaks	36
5.2 The protective effects of DMSO against double-strand breaks.....	37
5.3 Single giant DNA molecule's phase transition in the protocol of alcohol solutions.....	38
References	39
Curriculum Vitae	54
List of Publication	55

List of Figures

Figure 1.1 Schematic illustrations of a DNA double helix	56
Figure 1.2 Schematic illustrations of a double-strand breaks (DSBs).	57
Figure 1.3 A representative fluorescence image of DNA transition from elongated coil to compacted globule states (λ DNA)	58
Figure 1.4 Schematic of A-form, B-form and C-form DNA[57].....	59
Figure 2.1 the chemical formula of ascorbic acid.....	60
Figure 2.2 Example of the real-time observation of double-strand breaks. Fluorescence microscopic images on single T4 DNA molecule under photo-irradiation (left) and the corresponding quasi-three-dimensional profiles of the fluorescence-intensity distribution (right). (Fluorescent dye YOYO-1: 0.05 μ M, Ascorbic acid: 1.0 mM)	61
Figure 2.3 Photo-induced DSBs. (a) Time-dependence of the percentage of damaged DNA molecules. (b) Relationship between t^2 and $\log_{10}P$. (P is the percentage of surviving DNA molecules under photo-irradiation, which was calculated as [100% – (percentage of damaged DNA)])	62
Figure 2.4 Schematic illustrations of a double-strand break.....	63
(a) Two-step mechanism. (b) One-step mechanism.....	63
Figure 2.5 γ -ray-induced DSBs. (a) Fluorescence microscopic images of DNA molecules fixed on a glass surface after irradiation with different doses of γ -rays. (b) Average lengths of DNA, $\langle L \rangle$, vs. the irradiation dose of γ -rays. (c) Number	

of DSBs per DNA molecule, vs. the irradiation dose of γ -rays.	64
Figure 2.6 Ultrasound-induced DSBs. (a) Fluorescence microscopic images of DNA molecules fixed on a glass surface after exposure to ultrasound at different sound pressures. (b) Average lengths of DNA, $\langle L \rangle$, vs. the sound pressure of ultrasound. (c) Number of DNA double-strand breaks per molecule, $\langle n \rangle$, vs. the sound pressure of ultrasound.	65
Figure 2.7 Difference in the protective effect of AA. Vertical axis is the relative kinetic constant K/K_0 on the reaction to cause DSBs at different concentrations of ascorbic acid, where K_0 is the rate constant in the absence of AA. (For ultrasound-induced DNA damage, the kinetic constants are adapted from the threshold sound pressure, whereas the data are essentially the same for the kinetic parameters provided from the slopes, as shown in Fig.5c.).....	66
Figure 3.1 the chemical formula of DMSO	67
Figure 3.2 Example of the real-time observation of DSB caused by photo-irradiation-induced ROS. Fluorescence microscopic images of a single T4 DNA molecule under photo-irradiation (upper), and the corresponding quasi-three-dimensional profiles of the fluorescence intensity distribution (bottom). (Fluorescence dye: 0.05 μ M YOYO-1 in the absence of DMSO).	68
Figure 3.3 Photo-induced DSBs. (a) Time-dependence of the percentage of damaged DNA molecules at different DMSO concentrations. (b) The relationship between t_2 and $\log_{10}P$, where P is the percentage of surviving DNA molecules, which was calculated as $[100\% - (\text{percentage of damaged DNA})]$. (The kinetic constants,	

K_v 's (s^{-2}), are evaluated from the slopes of Figure 2b.) (For DMSO's concentration on 2% and 3%, fitting lines are coincided since their slopes are very close.)69

Figure 3.4 DSBs induced by γ -ray. (a) Fluorescence microscopic images of DNA molecules fixed on a glass surface after irradiation with different doses of γ -ray. (b) Average DNA lengths, $\langle L \rangle$, vs. the irradiation dose of γ -rays. (c) Number of DSBs per 10 kbp, $\langle n \rangle$, vs. the irradiation dose of γ -rays. (The kinetic constants, K_γ 's (Gy), are evaluated from the slopes of Figure 3c.) (As DMSO's concentration beyond 2%, fitting lines are coincided since their slopes are very close.)..... 70

Figure 3.5 Freezing-induced DSBs. (a) Single DNA image after freeze/thawing to -25°C (upper: slow frozen) and -80°C (lower: quick frozen). (b) Average lengths of DNA, $\langle L \rangle$, vs. the concentration of DMSO. (c) The number of DSBs per 10 kbp, $\langle n_f \rangle$, vs. the concentration of DMSO..... 71

Figure 3.6 Difference in the protective effect of DMSO. Vertical axis is the relative kinetic constant $k = K/K_0$ for the generation of DSBs at different concentrations of DMSO, where K_0 is the rate constant in the absence of DMSO. With respect to freezing, quickfreezing is to -80°C , and slow freezing is to -25°C 72

Figure 4.1 the chemical formula of (a) 1-propanol and (b) 2-propanol..... 73

Figure 4.2 Fluorescence images of representative styles of DNA molecules in solutions [propanol concentration of samples from up to blow: 0%, 50%, 80% (v/v) (1-propanol)]..... 74

Figure 4.3 After applied an electric field around ~ 10 V/cm to the DNA samples, the coiled and globular states separated..... 75

Figure 4.4 Distribution of long-axis length of DNA molecules in propanols solutions.	76
Figure 4.5 CD spectra of DNA (λ -DNA, 30 μ M in nucleotide units) at different propanol solutions.....	77
Figure 4.6 (a) The average long-axis length of DNA molecules at different alcohol solutions; (b) The globular rate of DNA samples at different propanol solutions; (c) Degrees of ellipticity (θ) of CD spectra of DNA samples at 270 nm	78

Acknowledgements

Firstly, I would like to express my sincere gratitude to my advisor Prof. Kenichi Yoshikawa for the continuous support of my study and related research, for his patience, motivation, and immense knowledge. His guidance helped me in all the time of research and writing of this thesis. I could not have imagined having a better advisor and mentor for my study.

Besides my advisor, I am also grateful to Prof. Yuko Yoshikawa and Prof. Tadahiro Kenmotsu. I am extremely thankful and indebted to them for sharing expertise, and sincere and valuable guidance and encouragement extended to me. I would also like to take this opportunity to express gratitude to all of the laboratory members for their help and support.

Last but not least, I would like to thank my family: my parents, my brother and Miss Jingwen Hu for supporting me spiritually throughout writing this thesis and my life in general.

Chapter 1

General Introduction

1.1 Research history of DNA

With the discovery of Deoxyribonucleic acid (DNA) by Johann Friedrich Miescher in 1869, many researches into DNA had already been done over past 150 years [1]. In the middle of the twentieth century, some of the most fundamental discoveries had been found in DNA research. During the previous period, proteins had been believed as the carrier of genetic information [2-3]. Oswald T. Avery, Colin MacLeod and Maclyn McCarty published their landmark paper in 1944 suggesting that it was DNA which carry the information of genetic [4]. A few years later, Erwin Chargaff discovered that the base composition of DNA varies between species. It is also found that within each species the bases are always present in fixed ratios: the same number of adenine as thymine bases and the same number of cytosine as guanine bases [5-6]. Alfred Hershey and Martha Chase confirmed DNA as the genetic material in 1952 [7]. After a year, building on X-ray analyses by Rosalind Franklin and Maurice Wilkins, Francis Crick and James Watson famously solved the structure of DNA [9]. Finally, by the middle of 1960s the genetic code had been cracked [10].

1.2 Basic structure of DNA

DNA plays a very important role in all living organisms since it is a fundamental biomolecule carrying genetic information. As shown in figure 1.1, there are two single-stranded polymers around each other forming as a double-helix structure. Both of these strands consist of a chain of basic building blocks, which contains a phosphate group, a deoxyribose sugar, and a nitrogenous base [11]. The stacking interaction between aromatic rings of adjacent bases and the specific hydrogen bonds between nitrogenous base pairs of opposite DNA strands are the two major forces responsible for the stability of the double-helix structure of DNA [11-13].

1.3 Double-strand breaks (DSBs) of DNA

Damage to DNA is a major problem for living things. DNA damage is currently categorized into 4 types: base changes, cross-linking, and single- and double-strand breaks (DSBs). Among these, DSBs (figure 1.2) are considered to be the most serious because they lead to cancer and cell death [14-19]. Many studies have been performed to detect DSBs both in vivo and in vitro. The polymerase chain reaction can be used to detect DNA damage through observation of the termination of amplification [20-21]. Immunological assays are also commonly used for the detection of oxidative DNA damage through the use of an antibody or immunoglobulin [20, 22]. In situ hybridization provides information on specific changes in certain DNA sequences [20, 23]. A comet assay can detect double-strand breaks in DNA, although a quantitative

evaluation is almost impossible [20, 24]. Despite the availability of these methods, it has been difficult to estimate the number of double-strand breaks in a reliable manner, especially for genome-sized long DNA molecules. Recently, it has been demonstrated that the direct visualization of single giant DNA molecules using fluorescence microscopy provide useful information on the structure and function of genomic DNA molecules [25-27], including the application to analyze DSBs in a quantitative manner [28-36].

1.4 High-order structure transition of DNA

DNA transition between elongated coil and compacted globule states, the coil-globule transition, represents one of the central problems in the field of biochemistry and biophysics. There are many previous studies have examined this problem both in theoretical and experimental [37-49]. A lot of these researches focus on linear polymer chains since it is the common style of DNA molecules in most living cells [37, 39-40, 42-43, 45-46, 48-49]. During the past couple of decades, it has been found that long DNA above the size of several tens kilo base pairs (kbp) exhibits unique conformational characteristics, as has been demonstrated by single molecular observation in bulk solutions with high sensitive fluorescence microscopy [38, 40, 43, 47].

1.5 Secondary structure of DNA

There are several secondary conformations of DNA molecules. The B-form which was described by Watson and Crick is common kind of DNA in cells [11]. It is 23.7 Å wide and extends 34 Å per 10 bp of sequence. The double helix makes one complete turn about its axis every 10.4-10.5 base pairs in solution. A-form is thought to be a biologically active double helical structure of DNA. It is a shorter, compact helical structure with a right-handed double helix similar to the B-form [50]. C-form is another possible double helical structure of DNA. It is also a right-handed double helix very similar to the B-form [51]. DNA secondary structure has close connections with life activities. It is reported that the secondary structure of DNA is a common and causative factor for expansion human disease and it also has influence on human telomerase activity [52-53]. There are a lot of researches had done on DNA's secondary structure in different chemicals solutions [54-56]. A-form, B-form and C-form are three DNA conformations which had been found in solutions [50-51]. Figure 1.4 are the schematic of A-form, B-form and C-form DNA [57]. B-form (in the middle) is the normal secondary structure of DNA in solutions. The compact style of DNA in the left is A-form. C-form DNA in the right is also right-handed.

1.6 Organizations of thesis

The remainder of the dissertation is organized as follows. Chapter 2 briefly describes

the protective effect of ascorbic acid on photo-, γ -ray and ultrasound-induced double-strand breaks of Giant DNA (T4 phage DNA:166 kbp). Chapter 3 summarizes the protective effect of ascorbic acid on photo-, γ -ray and freezing-induced DNA (T4 phage DNA:166 kbp) double-strand breaks. Chapter 4 briefly describes the high-order structure transition and secondary structure changes of genome-sized DNA (λ phage DNA:47 kbp) in different propanols solutions.

Chapter 2

Protective Effect of Ascorbic Acid against Double-strand Breaks in Giant DNA: Marked Differences among the Damage Induced by Photo-irradiation, Gamma-rays and Ultrasound

2.1 Introduction

Reactive oxygen species (ROS), which are generated through various processes, have been considered to be a major contributing factor to DNA strand breaks. The use of an antioxidant is an efficient method for protecting DNA from damage induced by reactive oxygen radicals [14, 58].

Ascorbic acid (AA), or vitamin C, is a representative antioxidant. Pauling claimed that AA could play a significant role in maintaining good health in humans [59-60]. It has been reported that AA can reduce ROS in human sperm cells to minimize the risk of DNA damage [61]. The chemical formula of AA was shown in figure 2.1.

In the present study, to evaluate the protective effects of AA on genome DNA molecules in a quantitative manner, we measured DSBs caused by photo-irradiation in the presence of sensitizer, γ -rays and ultrasound through single-molecule observation by fluorescence microscopy. To observe the effect of photo-induced reaction oxygen species, we used YOYO-1 (quinolinium,1,1'-[1,3-propanediyl-bis [(dimethylimino)-3,

1-propanediyl]] bis [4-[(3-methyl-2(3H)-benzoxazolylidene)-methyl]]-tetraiodide) as a photosensitizer to generate reactive oxygen, and performed the real-time observation of double-strand breaks in individual DNA molecules, where YOYO-1 also helps to visualize DNA as a fluorescence dye [30]. With regard to γ -ray and ultrasound, the numbers of DSBs were evaluated in terms of the average length of DNA molecules at different degrees of irradiation in the presence of AA.

2.2 Materials and Methods

2.2.1 Materials

T4 phage DNA (166 kbp, contour length 57 μ m) was purchased from Nippon Gene (Toyama, Japan). A fluorescent cyanine dye, YOYO-1 (quinolinium, 1, 1'-[1, 3-propanediyl-bis [[(dimethylimino)-3, 1-propanediyl]] bis [4-[(3-methyl-2(3H)-benzoxazolylidene)-methyl]]-tetraiodide), was purchased from Molecular Probes, Inc. (Oregon, USA). Antioxidants, 2-mercaptoethanol (2-ME) and AA, and other necessary chemicals were purchased from Wako Pure Chemical Industries (Osaka, Japan).

2.2.2 Real-time observation of photo-induced breakage

In fluorescence microscopic observations, to minimize intermolecular aggregation, measurements were conducted at a low DNA concentration (0.1 μ M in nucleotide units). T4 phage DNA was dissolved in buffer solution with YOYO-1 in 10

mM Tris-HCl (pH: 7.5). To evaluate the protective effects against double-strand breaks, AA was added to samples with final concentrations of 0.5 mM and 1.0 mM. 2-ME (concentration: 4% (v/v)) was added to the samples to slow the photo-cleavage reaction to a level that was suitable for real-time observation.

The double-strand damage in individual DNA molecules was observed at a peak emission wavelength of 510 nm under strong light illumination. Fluorescence DNA images were captured by use of an Axiovert 135 TV microscope (Carl Zeiss, Oberkochen, Germany) equipped with an oil-immersed 100x objective lens, and recorded on DVD through an EBCCD camera (Hamamatsu Photonics, Hamamatsu, Japan). The recorded videos were analyzed by VirtualDub, a free and open-source video-capture and video-processing utility for Microsoft Windows written by Avery Lee. All observations were carried out at around 20 °C [29-30].

2.2.3 Gamma-ray and ultrasound irradiation

T4 phage DNA (final concentration: 0.1 μ M) was dissolved in Tris-HCl (concentration: 10 mM) buffer solution at pH 7.5. After AA was added to the DNA solution at either 0.5 mM or 1.0 mM, the samples were irradiated by ^{60}Co γ -ray at a dose rate of 3860 Gy/h. The quantity of γ -rays was controlled by the duration of irradiation [30, 34].

Ultrasound for irradiation was provided by two Langevin transducers (FBL28452HS; FUJI CERAMICS, Fujinomiya, Japan) and the power was controlled by adjusting the transducers. The solutions for irradiation contained 0.1 μ M T4 DNA,

AA (final concentration: 1.0 mM) with 10 mM Tris-HCl buffer [31].

2.2.4 Measurement of the length of single DNA molecules by fluorescence microscopy

DNA molecules were fixed on a glass surface after the addition of YOYO-1 (final concentration: 1 μ M). In order to stretch DNA molecules, glasses were pre-treated with poly-(L-Lysine) (concentration: 0.05% (v/v)) solution, and washed repeatedly with distilled water. A droplet (15 μ l) of a sample was adsorbed on a modified glass slide and covered with a glass coverslip slightly. Fluorescence images were observed with an Axiovert 135 TV microscope (Carl Zeiss, Oberkochen, Germany) and analyzed by free software, ImageJ (National Institute of Mental Health, MD, USA) [30-31].

2.3. Results and Analysis

2.3.1 Protective effect of ascorbic acid against photo-induced DNA double-strand breaks

Figure 2.2 exemplifies the real-time observation of double-strand breaks and the corresponding quasi-three-dimensional profiles of the fluorescence-intensity distribution for a DNA molecule.

From the visual confirmation of breakage, the breakage time, τ , was evaluated by taking time zero as the moment when focused illumination was initiated. The

average breakage time, $\langle\tau\rangle$, was calculated from the data for 40-50 DNA molecules. In the absence of AA, $\langle\tau\rangle$ was 13 s. $\langle\tau\rangle$ increased with the addition of AA: $\langle\tau\rangle$ was 22 and 26 s in the presence of 0.5 and 1.0 mM AA, respectively. Figure 2.3a shows the time-dependent increase on the percentage of damaged DNA molecules under of the double-strand breaks under photo-irradiation.

In order to gain further insights into the mechanism of the double-strand breaks, as in Figure 2.3b, we rescaled the graph by placing the logarithm of the probability P of surviving DNA and the square of the duration of irradiation on the vertical and horizontal axes, respectively. The linear relationships in the figure implies that the kinetics is given as the multiplication of two independent events, i.e., the double-strand breaks are induced as a two-step mechanism as the result of occurrence of two single-strand breaks nearby each other on the both sides of double-stranded helix [29-30]. As illustrated in Figure 2.4a, in the two-step mechanism, single-strand breaks, or nicks, are generated randomly along double-strand DNA molecules under irradiation (Step 1). When another single-strand break occurs on the other DNA strand near a certain nick, a double-strand break (Step 2) is generated, which is recognized as fragmentation in the single-molecule measurement (Figure 2.2). A DNA chain is cut into fragments only when the sugar phosphate backbones on both sides are broken. We have previously reported the details of the kinetics of DSBs through such a two-step mechanism [29-30]. In the following discussion, we only describe the essence on the theoretical scheme to analyze the experimental data.

Under constant illumination with a power of I , the number of nicks along a

single DNA molecule will increase as in eq. (1), where α is a constant:

$$dn / dt = \alpha I \quad (2.1)$$

By denoting P as the probability of surviving DNA molecules against double-strand damage, the rate of the decrease in P can be represented as the product of n (number of nicks) and P :

$$dP / dt = -knP = -\alpha ItP \quad (2.2)$$

where k is a rate constant. Then, we obtain

$$\log_{10}(P/P_0) \propto -\alpha It^2 \quad (2.3)$$

By considering the initial condition as $P_0 = 1$ at $t = 0$, we obtain eq. (2.4):

$$\log_{10}(P) = -K^V t^2 \quad (2.4)$$

where K^V is a rescaled kinetic constant. Thus, the slopes in Figure 2.3b provide quantitative information on the protective effect of AA against photo-induced double-strand breaks.

The linear relationships in Figure 2.3b actually demonstrate the validity of eq.

(2.4) for photo-induced DSBs, and from such relationships we can evaluate the relative kinetic constant K^V / K^V_0 , where A_0 is the case without AA. The difference in the slopes in Figure 2.3b indicate that the kinetics on the double-strand breaks in the presence of 0.5 mM and 1.0 mM AA are about 40% and 30%, respectively, of those in the absence of AA. It is also to be noted that such protective effect of AA is expected to work for the kinetics of single-strand breaks, as suggested from the above mentioned theoretical framework.

2.3.2 Protective effect of ascorbic acid against gamma-ray-induced DNA double-strand breaks

Fluorescence images of DNA fixed on a glass substrate for specimens after γ -ray radiation are exemplified in figure 2.5a. As shown, the length of DNA molecules decreases with an increase in the intensity of γ -ray irradiation for both with and without AA. The average control length of DNA, $\langle L_0 \rangle$, was determined to be 20.3 μm for the samples without γ -ray radiation. This is somewhat smaller than the natural contour length (57 μm) and can be attributed to the procedure used to extract and purify T4 DNA molecules from the phage. Figure 2.5b shows the change in the average length $\langle L \rangle$ of DNA as a function of the irradiation dose. If the average number of DSBs per individual DNA molecule is defined as $\langle n \rangle$, the following relationship is derived under the assumption of a one-step mechanism (Figure 2.3b) [29-30]:

$$\langle n \rangle \approx \langle L_0 \rangle / \langle L \rangle - 1 \quad (2.5)$$

The proportionality of $\langle n \rangle$ with respect to the irradiation dose with γ -ray is shown in figure 2.5c. Thus, we assumed eq. (6) by introducing a kinetic constant K^γ :

$$n = K^\gamma D \quad (2.6)$$

2.3.3 Protective effect of ascorbic acid against ultrasound-induced DNA double-strand breaks

Figure 2.6a exemplifies the DNA observations after exposure to ultrasound. We analyzed the experimental data in the same manner as for γ -ray-induced double-strand breaks. Based on the data on the sound pressure level-dependence of the average length $\langle L \rangle$ given in figure 2.6b, we obtained a graph of the average number of breaks per original DNA molecule, $\langle n \rangle$, with respect to the sound pressure, as shown in figure 2.6c. This confirms the existence of a threshold value of sound pressure for DNA double-strand breaks; below this threshold, the probability of double-strand breaks is essentially zero [31]. Above the threshold, $\langle n \rangle$ increases linearly with the sound pressure. Interestingly, the nature of the increase in $\langle n \rangle$ is almost the same independent of the presence or absence of AA. These results demonstrate that AA does not have an obvious protective effect against ultrasound-induced DSBs.

As in the analysis of γ -ray-induced DSBs, the slope from the linear relationship

with the intercept of horizontal axis at the threshold sound pressure $p_0 = 40$ kPa, kinetic constant, K^U , is given as in eq. (2.7):

$$n = K^U(p - 40) \quad (2.7)$$

where n is the number of DNA double-strand breaks and p (kPa) is the sound pressure of the ultrasound.

2.3.4 Comparison of the protective effects of ascorbic acid among photo-irradiation, gamma-rays and ultrasound

To compare the protective effects of AA against DSBs due to irradiation from different sources based on the experimentally available kinetic constants, K^V , K^γ and K^U , we introduced a relative constant, $K_1 = K / K_0$, where K_0 is the kinetic constant of the control group for each radiation source. Thus, it becomes possible to compare the degree of protective effect by AA, regardless the mechanism of the DSBs, either one-step or two-step. Changes in the relative constant K_1 under different concentrations of AA are shown in figure 2.7.

AA decreased the DNA damage caused by the exposure to visible light (510nm) and this protective effect was enhanced with an increase in the concentration of AA. The DSBs induced by visible light decreased by about 65% in 1.0 mM AA solution. Although AA had a similar protective effect against γ -ray-induced DSBs, the damage was reduced by only around 30% in 1.0 mM AA solution, which is not as

good as the protective effect against photo-induced damage. On the other hand, AA did not have any obvious protective effect against DSBs caused by ultrasound, where the kinetic constant is essentially the same as that in the absence of AA.

2.4. Discussion

The protective effects of ascorbic acid against double-strand breaks in giant DNA molecules, which were caused by photo-irradiation in the presence of sensitizer, γ -rays and ultrasound, were tested at the level of single DNA molecules.

With regard to photo-induced DSBs, AA obviously reduced the number of breaks and this inhibitory effect increased with an increase in the AA. As for the DNA damage caused by γ -rays, the protective effect of AA is somewhat weaker compared to the case of photo-induced damage. On the contrary, for the damage by ultrasound, AA did not show any obvious protective effects against DSBs.

Previous studies have shown that there are two main mechanisms for the development of radiation-induced DSBs [29-30]. For γ -ray radiation, single step is the main process to cause DSBs (see figure 2.4b), which is attributed to the generation of number of ROS upon the incident of individual photon of γ -ray. Whereas photo-radiation causes DSBs through two step mechanism (figure 2.4a) by reflecting that each single photon causes mostly single ROS and thus induces only single strand break. Then, when a second single strand break occurs where near the existing single strand break, DBS is caused, i.e., the two step mechanism. Summarizing the results

and discussion we may conclude as that: 1) The significant protective effect of AA against photo-induced damage may reflect the effective diminish of ROS by AA. 2) For the γ -ray induced DSB, the protective effect by AA is a little bit weaker than the case of photo irradiation. This may be due to the generation of numbers of ROS by single photon of γ -ray. Surviving oxygen species against the diminishment effect by AA may cause DSBs. 3) As for the DSBs by ultrasound, damage is caused by the shockwave through the generation of cavitations [31]. Thus, the chemical effect of AA to diminish ROS is considered to be negligibly small for the protection of DSBs.

Chapter 3

Protective Effect of DMSO against Double-strand Breaks in Giant DNA: Differences among the Damage induced by Photo-and γ -ray-irradiation, and Freezing

3.1 Introduction

Dimethyl sulphoxide (DMSO) is known to be a useful free radical scavenger and a radio-protectant [62-69]. In fact, it has been reported that DMSO reduces the degree of radiation injury of adjacent organs in cancer radiotherapy. Radiation damage can be classified as direct or indirect [66,70]. In the indirect mechanism, the irradiation of organs as well as the cellular medium causes formation of chemically active species, i.e., reactive oxygen species (ROS), such as the hydroxyl radical and methyl radical [70-71]. However, the mechanism underlying chemical reduction of reactive species by DMSO is still unclear [62].

DMSO is one of the most important agents in cryopreservation, i.e., it protects living cells, organs, and tissues during storage at freezing temperatures [62-63, 72-81]. When the DSBs occur in the preserved cells, the damage is hazardous to the cell, and the viability after preservation will be significantly lower, because the cell will not survive during subsequent cell mitosis after thawing. This protective effect on DNA has been argued to be related to the strong solvation effect of DMSO on water molecules [63, 72-74, 82]. DMSO interacts with water molecules through the two

hydrogen bonds of water [81]. The chemical formula of AA was shown in figure 3.1.

Despite these useful practical applications of DMSO, the protective effect of DMSO against DSBs induced due to radiation or freezing/thawing has not yet been evaluated quantitatively. In the present study, to quantitatively evaluate the protective effects of DMSO against DSBs on genomic DNA molecules by use of single DNA observation, we artificially induced DSBs by several different injury sources; photo-induced reactive oxygen, γ -ray irradiation, and freeze/thawing. To observe the effect of photo-induced ROS, YOYO-1, a green fluorescent dye, was used as a photo sensitizer to generate ROS, and the real-time observation of DSBs in individual DNA molecules was performed, where YOYO-1 also helps to visualize DNA under visible light [83-86]. With regard to γ -ray irradiation, the number of DSBs was evaluated in terms of the average length of DNA molecules at different degrees of irradiation in the presence of DMSO. Likewise, we also evaluated the degree of DSBs caused by freezing/thawing—with two cold temperatures ($-25\text{ }^{\circ}\text{C}$ and $-80\text{ }^{\circ}\text{C}$)—by considering the phase boundary of freezing in a water-DMSO solution [78]. Because thermal disruption is one of the critical factors in cryopreservation, application of our method will provide a critical knowledge about freezing/thawing stress on preserved DNA.

3.2 Materials and Methods

3.2.1 Materials

T4 phage DNA (166 kbp) was purchased from Nippon Gene (Toyama, Japan). DMSO was obtained from Wako Pure Chemical Industries (Osaka, Japan). The fluorescent cyanine dye, YOYO-1 (quinolinium, 1,1'-[1,3-propanediyl-bis[(dimethylimino)-3,1-propanediyl]] bis[4-[(3-methyl-2(3H)-benzoxazolylidene)-methyl]]-tetraiodide), was purchased from ThermoFisher Scientific corporation (Waltham, MA). The antioxidants, 2-mercaptoethanol (2-ME) and DMSO, and other necessary chemicals, were purchased from Wako Pure Chemical Industries (Osaka, Japan).

3.2.2 Real-time observation of photo-induced breakage

In fluorescence microscopic observations, measurements were conducted at a low DNA concentration (0.1 μM in nucleotide units). T4 phage DNA (final concentration 0.1 μM) was dissolved in a solution containing 0.05 μM YOYO-1. The antioxidant 2-ME (4 (v/v)%) was added to the samples to retard the photo-cleavage reaction so as to detect the reaction rate of DSB by real-time observation. To observe the effect of photo-induced ROS, YOYO-1 was used as a photosensitiser to generate reactive oxygen, and the real-time observation of DSBs was performed in individual DNA molecules, where YOYO-1 also helped to visualise DNA DSBs in individual DNA molecules at different DMSO concentrations at a peak emission wavelength of 510 nm under light illumination at 450–490 nm. Fluorescence images of DNA molecules

were captured by using an Axiovert 135 TV (Carl Zeiss, Jena, Germany) microscope equipped with an oil-immersed 100 × objective lens and were recorded on a DVD through an EBCCD camera (Hamamatsu Photonics, Hamamatsu, Japan). All observations were carried out at room temperature (24 °C) [83].

3.2.3 Measurements of the contour length of DNA molecules to evaluate the injury caused by γ -ray and freezing

DNA solutions with different DMSO concentrations were irradiated with ^{60}Co γ -rays at a dose rate of 28 Gy/min. The quantity of γ -rays was controlled by the duration of irradiation^{19,43}. For the evaluation of freezing-induced DSB, DNA samples in a DMSO-water solution were frozen to -25 °C (freezing speed: ca. -0.4 K/min) and -80 °C (freezing speed: ca. -0.9 K/min) for 4 hours with electric freezers. They were then thawed at 4.2 °C (NIHON FREEZER, Tokyo, Japan) for about 12 hours.

Just before the measurements by fluorescence microscopy, DNA molecules were stained with YOYO-1 (final concentration: 0.05 μM). Glasses were pre-treated with poly-(L-lysine) (concentration: 0.05 (v/v) %) solution, and washed repeatedly with distilled water. A droplet (10 μL) of a sample was absorbed on a modified glass slide and covered with a glass cover slide under weak shear. Fluorescence images were observed with an Axiovert 135TV microscope (Carl Zeiss, Jena, Germany) and analysed using ImageJ software (National Institute of Mental Health, MD, USA) [83].

3.3 Results

3.3.1 Protective effect of DMSO against DSBs caused by photo-irradiation-induced ROS

First, the process of double-strand breakage was observed in T4 phage DNA (166 kbp) in real-time by labelling YOYO-1, a photosensitiser, that helped to visualise DNA under a fluorescence microscope (Figure 3.2). The three images reveal the DNA conformations in the bulk aqueous solution as observed under translational and intra-chain Brownian motion. The corresponding quasi-three-dimensional images of the individual photo were acquired for illustration of the fluorescence intensity distribution for the DNA molecule (bottom images, Figure 3.2). Thus, fluorescence microscopy made it possible to monitor the process of double-strand breakage in individual molecules. The breakage time, τ (0.20 sec in this example, Figure 3.2), was evaluated by taking time zero as the moment when focused illumination was initiated.

Subsequently, a time-dependent increase in photo-irradiation-induced DNA damage in the solution containing different concentrations of DMSO was evaluated by calculating the percentage of damaged DNA strands relative to the total observed strands (Figure 3.3a). Further, the graph was rescaled by placing the logarithm of the probability of surviving DNA, P , and the square of the irradiation duration, t^2 , on the vertical and horizontal axes, respectively. The linear correlation between the square of breakage time and $\log_{10}P$ in figure 3.3b suggested that the kinetics of double-strand breakage can be given as the product of two independent events, i.e., DSBs are

induced via a two-step mechanism as follows:

In case of single-strand breaks (SSBs), nicks are generated randomly along the double-stranded DNA molecules under irradiation, and fragmentation of a DNA molecule is induced by an additional SSB near an existing SSB [83]. We previously reported the details of the kinetics of DSBs through a similar two-step mechanism [83]. Under constant illumination with a power I , the number of nicks along a single DNA molecule will increase as shown in equation (3.1), where α is a positive constant:

$$dn/dt = \alpha I \quad (3.1)$$

After integration, by setting n (number of nicks) = 0 at $t = 0$, we obtain:

$$n = \alpha I t \quad (3.2)$$

By denoting P as the probability (percentage) of surviving DNA molecules against double-strand damage, the rate of the decrease in P can be represented as the product of n and P :

$$dP/dt = -knP = -k\alpha I t P \quad (3.3)$$

where k is the rate constant. Next, we obtained:

$$\log_{10}(P/P_0) \propto -\alpha I t^2 \quad (3.4)$$

and by introducing an initial constant of $P(t = 0) = 1$ at $t = 0$, we obtained:

$$\log_{10} P = -K_v t^2 \quad , \quad (3.5)$$

Where K_v is the rescaled kinetic constant. The linear relationships between the square of the time and $\log_{10}P$ in figure 3.3b confirm that the above-mentioned two-step reactions define the underlying mechanisms of DSBs caused by photo-induced ROS. From figure 3.3a and 3.3b, it was apparent that the protective effect increased with an increase in DMSO concentration and this effect was essentially maintained in DMSO concentrations higher than 2%. From the slope of the graph in figure 3.3b, the relative kinetic constant of the DSB reaction was deduced to be, $k = K_v / K_v^0$, where K_v^0 is the constant in the absence of DMSO. The relative kinetic constant, k , at different DMSO concentrations was calculated from the slope in figure 3.3b (See Figure 3.6).

3.3.2 Protective effect of DMSO against γ -ray-induced DSBs

Next, fluorescence images of the T4 DNA fixed on a glass substrate after variable γ -ray-irradiation doses (Gy) were obtained (figure 3.4a). As shown, the length of DNA molecules decreased with a higher level of γ -ray-irradiation. The average length of DNA in a single observation, $\langle L_0 \rangle$, was determined to be 30.2 μm for the control

sample before γ -ray-irradiation. For the target DNA strands, $\langle L \rangle$ was plotted for the irradiation doses (Figure 3.4b). The average number from the data for $\langle L \rangle$ and DSBs per individual DNA molecule, $\langle N_r \rangle$, were evaluated by using the following equation [83]:

$$\langle N_\gamma \rangle = \langle L_0 \rangle / \langle L \rangle - 1 \quad (3.6)$$

To compare the number of DSBs in a quantitative manner, a new parameter $\langle n \rangle$, the average number of DSBs per 10 kbp was introduced:

$$\langle n \rangle = \langle N_\gamma \rangle \cdot 10 / X_0 \quad (3.7)$$

Here, X_0 is the number of units (kbp) of DNA under control conditions, which was calculated by comparison with the natural contour length (57 μm , 166 kbp).

$$X_0 = (\langle L_0 \rangle \cdot 166) / 57 \quad (3.8)$$

As a result, the data of a linear correlation between $\langle n \rangle$ and irradiation dose, D , was obtained, suggesting that the increase in DSBs was proportional to the dose of γ -ray-irradiation (Figure 3.4c). This linearity implies that the DSBs induced by γ -ray are caused in a single-step reaction, i.e., one DSB is caused by a single γ -ray photon. In contrast, in the ROS attack emitted from the fluorescence dye under visible-light

irradiation, one DSB was caused by a pair of neighbouring SSBs on complementary strands [83]. In this figure, the slope, K_γ , represents the kinetic constant under the framework of a one-step reaction mechanism. As shown in figure 3.4c, K_γ decreases monotonously with an increase in DMSO concentration up to 2% and was kept almost constant with a further increase in the concentration. Thus, the protective effect reached a plateau at 2% DMSO concentration.

3.3.4 Protective effect of DMSO against freezing-induced DSBs

Finally, DSBs caused by freeze/thawing in the solution containing variable DMSO concentrations were assessed by fluorescence microscopy using the DNA fixed on a solid substrate (Figure 3.5a). Further, the average length at different DMSO concentrations for freezing at $-25\text{ }^\circ\text{C}$ (slow frozen) and $-80\text{ }^\circ\text{C}$ (quick-frozen) were measured (Figure 3.5b). By using a method similar to that used to assess the γ -ray-induced DSBs, the relationship between the number of DSBs per 10 kbp, $\langle n_j \rangle$, and the DMSO concentration was obtained (Figure 3.5c). As shown, the probability of DSBs was higher for freezing to $-25\text{ }^\circ\text{C}$ than for quick freezing to $-80\text{ }^\circ\text{C}$ [87]. DMSO was found to have a protective effect against DSBs and significantly, this effect reached a plateau at 2% DMSO. Like the protective effects of DMSO against damage caused by photo-induced ROS and γ -ray-irradiation, the protective effect of DMSO against freezing-induced damage was maximum at a 2% concentration.

3.4 Discussion

In the current study, we induced DSBs in the target DNA using different sources and assessed DSBs directly by observing under a fluorescent microscope. The data provided the common kinetics of DSB formation by the variable resources.

To compare the protective effects of DMSO against DSBs, caused due to damage by different sources, based on experimentally available kinetic constants, K_v , K_γ , and K_f ; n_f , we introduced a relative constant, $k = K/K_0$, where K_0 is the kinetic constant of the control group for each injury source in the absence of DMSO. Using this renormalized constant k , it is possible to compare the degree of the protective effect of DMSO, regardless of any difference in the mechanism of double-strand breakage, including whether the mechanism involves either one-step or two-step reactions. Changes in the relative kinetic constant, k , under different concentrations of DMSO are summarized in figure 3.6. The DSBs caused by photo- and γ -ray-irradiation significantly decrease to the order of 1/100 when the concentration of DMSO is above 1.5–2.0%. In contrast, the decrease in the rate constant of DSBs remains in the order of 1/5–1/10 for injury due to freeze/thawing, even at a DMSO concentration $> 2\%$. This large difference in protection is attributable to the difference in the physical-chemical mechanism of DSBs. Considering freezing, the growth of ice crystals is considered to be the main cause of DSBs, and vitrification is critical for preservation [88-91]. However, when DMSO is added to an aqueous solution, the ice crystallization is expected to reduce, and thus the double-strand breakage would be decreased. On the contrary, γ -ray-irradiation is considered to cause DSBs mainly through an indirect mechanism, i.e., generated ROS may attack DNA molecules. It has been reported that a single γ -ray photon can produce several reactive species, which produce a DSB in a one-step process. For damage caused by photo-irradiation,

DSBs are induced mainly through a two-step mechanism. Interestingly, DMSO has a strong protective effect against ROS, regardless of whether the mechanism is single-step or two-step.

The protective effects of DMSO against photo- and γ -ray-irradiation were about 1.2-fold less than that against freeze-thawing. This difference between radical protection and freezing protection is attributable to the different mechanisms of radical damage (photo- and γ -ray-irradiation) and physical damage (freeze/thawing). Since DSBs are one of the most important types of DNA damage and the results of our experiment demonstrated that DMSO could decrease both physically and chemically induced DSBs, DMSO should be very effective in protecting DNA molecules from DSBs. As past research demonstrated that high concentration (more than 10%) of DMSO had various effects on biological systems, which was very toxic [67,69,72,78], the results from our experiment suggested that 2% DMSO would be a good starting point in future experiments in biological and medical sciences as well as cryopreservation.

The single-DNA observation provided precise kinetic data, and therefore, it is useful for quantitatively evaluating DSBs and is expected to be useful for measurements of DSBs caused by other types of injuries.

Chapter 4

Specific structural changes of DNA molecule in various alcohol solutions

4.1 Introduction

DNA transition between elongated coil and compacted globule states, the coil-globule transition, represents one of the central problems in the field of biochemistry and biophysics. There are many previous studies have examined this problem both in theoretical and experimental [37-49]. A lot of these researches focus on linear polymer chains since it the common style of DNA molecules in most living cells [37, 39-40, 42-43, 45-46, 48-49]. During the past couple of decades, it has been found that long DNA above the size of several tens kilo base pairs (kbp) exhibits unique conformational characteristics, as has been demonstrated by single molecular observation in bulk solutions with high sensitive fluorescence microscopy [38, 40, 43, 47].

There are several secondary conformations of DNA molecules. The B-form which was described by Watson and Crick is common kind of DNA in cells [11]. It is 23.7 Å wide and extends 34 Å per 10 bp of sequence. The double helix makes one complete turn about its axis every 10.4-10.5 base pairs in solution. A-form is thought to be a biologically active double helical structure of DNA. It is a shorter, compact helical structure with a right-handed double helix similar to the B-form [50]. C-form

is another possible double helical structure of DNA. It is also a right-handed double helix very similar to the B-form [51]. DNA secondary structure has close connections with life activities. It is reported that the secondary structure of DNA is a common and causative factor for expansion human disease and it also has influence on human telomerase activity [52-53]. There are a lot of researches had done on DNA's secondary structure in different chemicals solutions [54-56]. A-form, B-form and C-form are three DNA conformations which had been found in solutions [50-51]. Figure 1.4 are the schematic of A-form, B-form and C-form DNA [57].

DNA secondary structure has close connections with life activities. A-form, B-form and C-form are three DNA conformations which had been found in solutions [50-51,92].

In biomedical experiment, alcohol precipitation is a widely used technique to purify or concentrate nucleic acids [93-105]. Isopropanol (2-propanol) is one kind of alcohol often used to isolate DNA molecules from cells through the generation of precipitation [105-107]. Since the oxygen atoms and the nitrogen atoms in the backbone of DNA made it as a polar molecule, the polarity of solution should have influence on the high order structure of DNA. 1-propanol is always used as a solvent in the pharmaceutical industry mainly for resins and cellulose esters [106-107]. As 2- and 1-propanol are isomers with different polarity, we did the comparative study of the effect on the higher order structure of giant DNA between them through single-molecule by fluorescence microscopy. The chemical formula of 1-propanol and 2-propanol were shown in figure 4.1.

In this study, the high-order structure of giant DNA was evaluated through fluorescence microscope. The long-axis length of DNA molecules, parameter used to determine the high-order structure, showed huge difference between 1-propanol and 2-propanol solutions, which demonstrate that the high-order structure of DNA molecules will be influenced by the kinds of alcohol-water clusters of solutions. We also used the circular dichroism (CD) spectra to test the secondary structure of DNA. The results of degrees of ellipticity (θ) of DNA solutions in different propanols are also very different, which indicated that the kinds of alcohol-water clusters of solutions will also influence the secondary structure of DNA.

4.2 Materials and Methods

4.2.1 Materials

The bacteriophage λ -DNA (48 kbp) was purchased from Nippon Gene. A fluorescent cyanine dye, YOYO-1 (quinolinium, 1, 1'-[1, 3-propanediyl-bis [[dimethylimino)-3, 1-propanediyl]] bis [4 - [(3 - methyl - 2(3H) - benzoxazolylidene) - methyl]] - tetraiodide), was purchased from Molecular Probes, Inc. (Oregon, USA). Antioxidants, 2-mercaptoethanol (2-ME) was purchased from Wako Pure Chemical Industries (Osaka, Japan).

4.2.2 Single molecule observation of DNA through fluorescence microscope

DNA samples were dissolved in propanol-water solution with a final

concentration of 30 μM in nucleotide units. The YOYO-1 (final concentration: 1 μM) was added to the DNA solution, together with the antioxidant 4% (v/v) 2-ME. Fluorescence DNA images were captured by use of an Axiovert 135 TV microscope (Carl Zeiss, Oberkochen, Germany) equipped with an oil-immersed 100x objective lens, and recorded on DVD through an EBCCD camera (Hamamatsu Photonics, Hamamatsu, Japan). The recorded videos were analyzed by free software, VirtualDub (written by Avery Lee) and ImageJ (National Institute of Mental Health, MD, USA). All observations were carried out at around 24 °C.

4.2.3 Measurement of DNA secondary structure through circular dichroism (CD) spectra

Same DNA samples in propanol-water solution were prepared. In order to understand the change in the secondary structure of DNA depending on 1-propanol and 2-propanol concentration, the CD spectra of λ -DNA were measured with a CD spectrometer (J-820, JASCO, Japan). Measurements were performed at a scan rate of 100 nm/min and 2000 μL of each sample were tested at around 24 °C. The cell path length was 1 cm and CD spectra were obtained as the accumulation of three scans.

4.3 Results

4.3.1 High-order structure of DNA molecules in propanols solutions

For evaluating the coil status of DNA molecules, we measure the long-axis length of them, L , as fluorescence images and schematics of figure 1 showed. Fluorescence images of DNA molecules [propanol concentration of samples from up to blow: 0%,

50%, 70% (v/v) (1-propanol)] of figure 1 are three representative styles of DNA molecules in solutions. Figure 4.2(a) indicates λ -DNA exhibit a coil-globule coexisting state as partial globule. As shown in figure 4.3, after applied an electric field around 10 V/cm to the DNA samples [5], the bright spot separated and connect with a narrow bright line which indicated that coiled and globular states coexist in a single DNA molecule.

Figure 4.4 shows the distribution of long-axis length of DNA molecules. It could find that DNA molecules' globular state appeared when its long axis length less than 2.5 μm . The globular state became more as the long-axis length getting shorter. When long-axis length got shorter than 1.0 μm , DNA molecules exist as globule or coil-globule states. The pure coiled state of DNA almost disappeared. The average long-axis length is showed in figure 4.6(a). For DNA molecules in different concentrations of 1-propanol solutions, one minima of average length appear at 60 % (v/v). In 2-propanol solutions, the average long-axis length of DNA decreased and transited from elongated coil state to folded globule is generated around 70-80% (v/v). Above 75% (v/v), DNA maintained as folded globule and the average length of DNA molecules remains essentially the constant. As for the globular rate of DNA samples, figure 4.6(b) indicated that it basically increased with concentration of propanol increased. In 1-propanol solutions above 60% (v/v), the globular rate decreased a bit after the minima of average long-axis length of DNA samples.

4.3.2 Secondary structure of DNA molecules in propanols solutions

As spectra results showed in figure 4.5, for DNA molecules in 1-propanol solutions, from the positive band at around 275 nm and the negative band at around 245 nm, the secondary structure of DNA kept as B-like form from 0% to 70% (v/v). The spectra became really close to zero when concentration of 1-propanol is higher than 70% (v/v). It could be considered that it would not be successful in measuring the CD spectra of samples because of the deposition of DNA molecules. As for samples in 2-propanol solutions, the secondary structure changed to A-like form from 30% to 60% (v/v) since the positive band is higher and the negative band is lower than samples in 0 % (v/v). DNA molecules' secondary structure went back to B-like form at around 70% (v/v) of 2-proanol as the spectra result is close to 0%. By the reason of DNA deposition, it is also not successful in measuring the CD spectra of samples when the concentration of 2-propanol is higher than 75% (v/v). In order to understand DNA molecules' secondary structure clearly, degrees of ellipticity (θ) at 270 nm were showed in figure 4.6(c). It could be found that results of CD spectra measurement of 1-propanol and 2-propanol are quite different. DNA molecules in 1-propanol only showed B-like form before DNA deposition. In 2-propanol solution, both A-like and B-like form appeared when the concentration of 2-propanol lower than the DNA deposition concentration.

4. Discussion

The long-axis length of DNA molecules in solutions decreased as the concentration of

1-propanol increased to 60% (v/v), then increased a bit and keep it as the concentration getting higher. For 2-propanol solutions, the long-axis length just decreased as the concentration getting higher and then kept in the minimum in the high concentration. As shown in figure 4.6(a), for DNA in ethanol solutions, which is another common chemical used in DNA precipitation, the long-axis length reached a minimum at 60% (v/v), then increased as the concentration is getting higher [37].

The secondary-structure of DNA molecules kept as B-like form in 1-propanol solutions. However, it changed to A-like form and then back to B-like form in 2-propanol solutions as the concentration of 2-propanol increased. Moreover, past research of our group on the secondary-structure of DNA in ethanol solutions demonstrated that DNA showed B-, C- and A-like form as the concentration of ethanol getting higher [37]. The observed large difference of the effect of ethanol and propanol isomers on the DNA conformation will be discussed in relation to the nano-structure of alcohol solution.

Nowadays, structural characterization of genomic DNA is one of the most important trends in medicine, biology and agricultural sciences. The indispensable procedure for the analysis of DNA in living cells is to isolate DNA molecules as precipitates from the crude mixture in rich variety of cellular components. According to the standard experimental protocol in molecular biology and medicinal chemistry, usage of 2-propanol is recommended, seemingly without any reasonable physic-chemical explanation why 2-propanol is desirable [100-101]. As a related phenomenon, we have recently reported that ethanol causes reentrant transition on

DNA accompanied by the increase of its concentration [37]. We will discuss the mechanism of the reentrant transition in terms of the effect of nano-sized clusters on the ethanol, 1- and 2-propanol solutions with high concentrations.

DNA is negatively charged because of the negatively charged phosphate group in its structure. As all of alcohol molecules are polar, it could be inferred that the alcohol solutions will have influence on the structure of DNA molecules. Since alcohol molecules will combine with water molecules as cluster which are also polar, they will therefore affect DNA's structure. Many studies had been done on the formation of clusters in solutions of alcohols in water [108-113]. Previous study indicated that the clusters formation at composition of 1 alcohol molecule and 5 water molecules occur in 1-propanol and 2-propanol solutions. However, a composition of 5 1-propanol molecules and 40 water molecules cluster formation also showed in the mixture of 1-propanol and water [113]. The reentrant of DNA molecules' high-order structure could attribute to the special cluster showed in 1-propanol solution. The A-form secondary structure of DNA showed in the dehydration environment [50]. As the clusters in propanol are mainly the composition of 1 alcohol molecule and 5 water molecules, it could be the reason of the change of DNA secondary structure in 2-propanol solutions.

Chapter 5

General Conclusion

5.1 The protective effects of ascorbic acid against double-strand breaks

The protective effects of ascorbic acid against double-strand breaks in giant DNA molecules, which were caused by photo-irradiation in the presence of sensitizer, γ -rays and ultrasound, were tested at the level of single DNA molecules.

With regard to photo-induced DSBs, AA obviously reduced the number of breaks and this inhibitory effect increased with an increase in the AA. As for the DNA damage caused by γ -rays, the protective effect of AA is somewhat weaker compared to the case of photo-induced damage. On the contrary, for the damage by ultrasound, AA did not show any obvious protective effects against DSBs.

Summarizing the results we may conclude as that: 1) The significant protective effect of AA against photo-induced damage may reflect the effective diminish of ROS by AA. 2) For the γ -ray induced DSB, the protective effect by AA is a little bit weaker than the case of photo irradiation. This may be due to the generation of numbers of ROS by single photon of γ -ray. Surviving oxygen species against the diminishment effect by AA may cause DSBs. 3) As for the DSBs by ultrasound, damage is caused by the shockwave through the generation of cavitations. Thus, the chemical effect of AA to diminish ROS is considered to be negligibly small for the

protection of DSBs.

5.2 The protective effects of DMSO against double-strand breaks

The protective effects of DMSO against double-strand breaks in giant DNA molecules, which were caused by photo-irradiation in the presence of sensitizer, γ -rays and freezing, were tested at the level of single DNA molecules.

The DSBs caused by photo- and γ -ray-irradiation significantly decrease to the order of 1/100 when the concentration of DMSO is above 1.5–2.0%. In contrast, the decrease in the rate constant of DSBs remains in the order of 1/5–1/10 for injury due to freeze/thawing, even at a DMSO concentration $> 2\%$. This large difference in protection is attributable to the difference in the physical-chemical mechanism of DSBs. Considering freezing, the growth of ice crystals is considered to be the main cause of DSBs, and vitrification is critical for preservation. However, when DMSO is added to an aqueous solution, the ice crystallization is expected to reduce, and thus the double-strand breakage would be decreased. On the contrary, γ -ray-irradiation is considered to cause DSBs mainly through an indirect mechanism, i.e., generated ROS may attack DNA molecules. It has been reported that a single γ -ray photon can produce several reactive species, which produce a DSB in a one-step process. For damage caused by photo-irradiation, DSBs are induced mainly through a two-step mechanism. Interestingly, DMSO has a strong protective effect against ROS, regardless of whether the mechanism is single-step or two-step.

The protective effects of DMSO against photo- and γ -ray-irradiation were about 1.2-fold less than that against freeze-thawing. This difference between radical protection and freezing protection is attributable to the different mechanisms of

radical damage (photo- and γ -ray-irradiation) and physical damage (freeze/thawing). Since DSBs are one of the most important types of DNA damage and the results of our experiment demonstrated that DMSO could decrease both physically and chemically induced DSBs, DMSO should be very effective in protecting DNA molecules from DSBs.

5.3 Single giant DNA molecule's phase transition in the protocol of alcohol solutions

The long-axis length of DNA molecules in solutions decreased as the concentration of 1-propanol increased to 60% (v/v), then increased a bit and kept it as the concentration getting higher. For 2-propanol solutions, the long-axis length just decreased as the concentration getting higher and then kept in the minimum in the high concentration. As showed in figure 4.6(a), for DNA in ethanol solutions, which is another common chemical used in DNA precipitation, the long-axis length reached a minimum at 60% (v/v), then increased as the concentration getting higher [37].

The secondary-structure of DNA molecules kept as B-like form in 1-propanol solutions. However, it changed to A-like form and then back to B-like form in 2-propanol solutions as the concentration of 2-propanol increased. Moreover, past research of our group on the secondary-structure of DNA in ethanol solutions demonstrated that DNA showed B-, C- and A-like form as the concentration of ethanol getting higher [37]. The observed large difference of the effect of ethanol and propanol isomers on the DNA conformation will be discussed in relation to the nano-structure of alcohol solution.

References

- [1]. Miescher, F. "Letter I; to Wilhelm His; Tübingen, February 26, 1869 In: W." *Die Histochemischen und Physiologischen Arbeiten von Friedrich Miescher—Aus dem wissenschaftlichen Briefwechsel von F. Miescher* 1 (1869): 33-38.
- [2]. Dahm, Ralf. "Friedrich Miescher and the discovery of DNA." *Developmental biology* 278, no. 2 (2005): 274-288.
- [3]. Dahm, Ralf. "Discovering DNA: Friedrich Miescher and the early years of nucleic acid research." *Human genetics* 122, no. 6 (2008): 565-581.
- [4]. MacLeod, Avery OT, and Maclyn McCarty. "Studies of the chemical nature of the substance inducing transformation of pneumococcal types. induction of transformation by a deoxyribonucleic acid fraction isolated from pneumococcus type iii." *Journal of Experimental Medicine* 79 (1944): 137-158.
- [5]. Chargaff, Erwin, Ernst Vischer, Ruth Doniger, Charlotte Green, and Fernanda Misani. "The composition of the desoxyribose nucleic acids of thymus and spleen." *Journal of Biological Chemistry* 177, no. 1 (1949): 405-416.
- [6]. Chargaff, Erwin. "Structure and function of nucleic acids as cell constituents." In *Federation proceedings*, vol. 10, no. 3, p. 654. 1951.
- [7]. Hershey, Alfred D., and Martha Chase. "Independent functions of viral protein and nucleic acid in growth of bacteriophage." In *Die Entdeckung der Doppelhelix*, pp. 121-139. Springer Spektrum, Berlin, Heidelberg, 2017.
- [8]. Watson, James D., and Francis HC Crick. "Molecular structure of nucleic acids." *Nature* 171, no. 4356 (1953): 737-738.

- [9]. Davies, Kevin. *Cracking the genome: inside the race to unlock human DNA*. JHU Press, 2002.
- [11]. Watson, James D., and Francis HC Crick. "The structure of DNA." *Cold Spring Harbor symposia on quantitative biology*. Vol. 18. Cold Spring Harbor Laboratory Press, 1953.
- [12]. Watson, James D., and Francis HC Crick. "Genetical implications of the structure of deoxyribonucleic acid." *Nature* 171.4361 (1953): 964-967.
- [13]. Ornstein, Rick L., et al. "An optimized potential function for the calculation of nucleic acid interaction energies I. Base stacking." *Biopolymers* 17.10 (1978): 2341-2360.
- [14]. Loft, Steffen, and Henrik E. Poulsen. "Cancer risk and oxidative DNA damage in man." *Journal of molecular medicine* 74, no. 6 (1996): 297-312.
- [15]. Weinert, Ted. "DNA damage and checkpoint pathways." *Cell* 94, no. 5 (1998): 555-558.
- [16]. Fenech, Michael. "Chromosomal damage rate, aging, and diet." *Annals of the New York Academy of Sciences* 854, no. 1 (1998): 23-36.
- [17]. Rich, Tina, Rachel L. Allen, and Andrew H. Wyllie. "Defying death after DNA damage." *Nature* 407, no. 6805 (2000): 777.
- [18]. Bradbury, J. M., and S. P. Jackson. "The complex matter of DNA double-strand break detection." (2003): 40-44.
- [19]. Hoeijmakers, Jan HJ. "DNA damage, aging, and cancer." *New England Journal of Medicine* 361, no. 15 (2009): 1475-1485.

- [20]. Kumari, Sunita, Rajesh P. Rastogi, Kanchan L. Singh, Shailendra P. Singh, and Rajeshwar P. Sinha. "DNA damage: detection strategies." *EXCLI J* 7 (2008): 44-62.
- [21]. Schochetman, Gerald, Chin-Yih Ou, and Wanda K. Jones. "Polymerase chain reaction." *The Journal of infectious diseases* 158, no. 6 (1988): 1154-1157.
- [22]. Amaro, Ana M., Kevin B. Hallberg, E. Börje Lindström, and Carlos A. Jerez. "An immunological assay for detection and enumeration of thermophilic biomining microorganisms." *Applied and environmental microbiology* 60, no. 9 (1994): 3470-3473.
- [23]. McFadden, Geoffrey Ian. "In situ hybridization." In *Methods in cell biology*, vol. 49, pp. 165-183. Academic Press, 1995.
- [24]. Liao, Wenjuan, Michael A. McNutt, and Wei-Guo Zhu. "The comet assay: a sensitive method for detecting DNA damage in individual cells." *Methods* 48, no. 1 (2009): 46-53.
- [25]. Estevez-Torres, Andre, and Damien Baigl. "DNA compaction: fundamentals and applications." *Soft Matter* 7, no. 15 (2011): 6746-6756.
- [26]. Lundberg, Dan, Nikolay V. Bereznoy, Chenning Lu, Nikolay Korolev, Chun-Jen Su, Viveka Alfredsson, Maria da Graca Miguel, Björn Lindman, and Lars Nordenskiöld. "Interactions between cationic lipid bilayers and model chromatin." *Langmuir* 26, no. 15 (2010): 12488-12492.
- [27]. Zinchenko, Anatoly A. "Templating of inorganic nanomaterials by biomacromolecules and their assemblies." *Polymer Science Series C* 54, no. 1

(2012): 80-87.

- [28]. Kurita, Hirofumi, Tatsuya Takata, Hachiro Yasuda, Kazunori Takashima, and Akira Mizuno. "A kinetic analysis of strand breaks on large DNA induced by cigarette smoke extract." *Chemical Physics Letters* 493, no. 1-3 (2010): 165-169.
- [29]. Yoshikawa, Yuko, Mari Suzuki, Norihiro Yamada, and Kenichi Yoshikawa. "Double - strand break of giant DNA: protection by glucosyl - hesperidin as evidenced through direct observation on individual DNA molecules." *FEBS letters* 566, no. 1-3 (2004): 39-42.
- [30]. Yoshikawa, Yuko, Toshiaki Mori, Mari Suzuki, Tadayuki Imanaka, and Kenichi Yoshikawa. "Comparative study of kinetics on DNA double-strand break induced by photo-and gamma-irradiation: Protective effect of water-soluble flavonoids." *Chemical Physics Letters* 501, no. 1-3 (2010): 146-151.
- [31]. Yoshida, Kenji, Naoki Ogawa, Yukihiro Kagawa, Hiraku Tabata, Yoshiaki Watanabe, Takahiro Kenmotsu, Yuko Yoshikawa, and Kenichi Yoshikawa. "Effect of low-frequency ultrasound on double-strand breaks in giant DNA molecules." *Applied Physics Letters* 103, no. 6 (2013): 063705.
- [32]. Shimobayashi, Shunsuke F., Takafumi Iwaki, Toshiaki Mori, and Kenichi Yoshikawa. "Probability of double-strand breaks in genome-sized DNA by γ -ray decreases markedly as the DNA concentration increases." *The Journal of chemical physics* 138, no. 17 (2013): 05B604_1.
- [33]. Yoshikawa, Yuko, Mari Suzuki, Ning Chen, Anatoly A. Zinchenko, Shizuaki Murata, Toshio Kanbe, Tonau Nakai, Hidehiro Oana, and Kenichi Yoshikawa.

- "Ascorbic acid induces a marked conformational change in long duplex DNA." *The FEBS Journal* 270, no. 14 (2003): 3101-3106.
- [34]. Suzuki, Mari, Cecile Crozatier, Kenichi Yoshikawa, Toshiaki Mori, and Yuko Yoshikawa. "Protamine-induced DNA compaction but not aggregation shows effective radioprotection against double-strand breaks." *Chemical Physics Letters* 480, no. 1-3 (2009): 113-117.
- [35]. Yoshikawa, Yuko, Naoki Umezawa, Yuki Imamura, Toshio Kanbe, Nobuki Kato, Kenichi Yoshikawa, Tadayuki Imanaka, and Tsunehiko Higuchi. "Effective chiral discrimination of tetravalent polyamines on the compaction of single DNA molecules." *Angewandte Chemie International Edition* 52, no. 13 (2013): 3712-3716.
- [36]. Iwaki, Takafumi, Tomomi Ishido, Ken Hirano, Alexei A. Lazutin, Valentina V. Vasilevskaya, Takahiro Kenmotsu, and Kenichi Yoshikawa. "Marked difference in conformational fluctuation between giant DNA molecules in circular and linear forms." *The Journal of Chemical Physics* 142, no. 14 (2015): 04B604_1.
- [37]. Simpson, Robert T., Fritz Thoma, and Joel M. Brubaker. "Chromatin reconstituted from tandemly repeated cloned DNA fragments and core histones: a model system for study of higher order structure." *Cell* 42.3 (1985): 799-808.
- [38]. Ueda, Masanori, and Kenichi Yoshikawa. "Phase transition and phase segregation in a single double-stranded DNA molecule." *Physical review letters* 77.10 (1996): 2133.
- [39]. Bloomfield, Victor A. "DNA condensation by multivalent cations." *Biopolymers*

44.3 (1997): 269-282.

- [40]. Tang, M. X., and F. C. Szoka. "The influence of polymer structure on the interactions of cationic polymers with DNA and morphology of the resulting complexes." *Gene therapy* 4.8 (1997).
- [41]. Yamasaki, Yuichi, and Kenichi Yoshikawa. "Higher order structure of DNA controlled by the redox state of Fe²⁺/Fe³⁺." *Journal of the American Chemical Society* 119.44 (1997): 10573-10578.
- [42]. Bednar, Jan, et al. "Nucleosomes, linker DNA, and linker histone form a unique structural motif that directs the higher-order folding and compaction of chromatin." *Proceedings of the National Academy of Sciences* 95.24 (1998): 14173-14178.
- [43]. Daban, Joan-Ramon. "Physical constraints in the condensation of eukaryotic chromosomes. Local concentration of DNA versus linear packing ratio in higher order chromatin structures." *Biochemistry* 39.14 (2000): 3861-3866.
- [44]. Yoshikawa, Kenichi. "Controlling the higher-order structure of giant DNA molecules." *Advanced drug delivery reviews* 52.3 (2001): 235-244.
- [45]. Dias, Rita S., et al. "Coil– globule transition of DNA molecules induced by cationic surfactants: A dynamic light scattering study." (2005).
- [46]. Woodcock, Christopher L., and Rajarshi P. Ghosh. "Chromatin higher-order structure and dynamics." *Cold Spring Harbor perspectives in biology* 2.5 (2010): a000596.
- [47]. Oda, Yuki, et al. "Highly Concentrated Ethanol Solutions: Good Solvents for

- DNA as Revealed by Single - Molecule Observation." *ChemPhysChem* 17.4 (2016): 471-473.
- [48]. Lyubchenko, Y. L., et al. "Atomic force microscopy of DNA and bacteriophage in air, water and propanol: the role of adhesion forces." *Nucleic acids research* 21.5 (1993): 1117-1123.
- [49]. Schaper, Achim, J. P. Starink, and Thomas M. Jovin. "The scanning force microscopy of DNA in air and in n - propanol using new spreading agents." *FEBS letters* 355.1 (1994): 91-95.
- [50]. Arnott, Struther, and D. W. L. Hukins. "Optimised parameters for A-DNA and B-DNA." *Biochemical and biophysical research communications* 47.6 (1972): 1504-1509.
- [51]. Arnott, Struther, and Erik Selsing. "The conformation of C-DNA." *Journal of molecular biology* 98.1 (1975): 265IN47267-266269.
- [52]. Fletcher, Terrace M., et al. "Effect of DNA secondary structure on human telomerase activity." *Biochemistry* 37.16 (1998): 5536-5541.
- [53]. McMurray, Cynthia T. "DNA secondary structure: a common and causative factor for expansion in human disease." *Proceedings of the National Academy of Sciences* 96.5 (1999): 1823-1825.
- [54]. Brahms, J., and W. F. H. M. Mommaerts. "A study of conformation of nucleic acids in solution by means of circular dichroism." *Journal of molecular biology* 10.1 (1964): 73-88.
- [55]. Tunis-Schneider, Mary Jane B., and Marcos F. Maestre. "Circular dichroism

- spectra of oriented and unoriented deoxyribonucleic acid films—a preliminary study." *Journal of molecular biology* 52.3 (1970): 521-541.
- [56]. Zimmer, Christoph. "Effects of the antibiotics netropsin and distamycin A on the structure and function of nucleic acids." *Progress in nucleic acid research and molecular biology* 15 (1975): 285-318.
- [57]. Lu, Xiang - Jun, and Wilma K. Olson. "3DNA: a software package for the analysis, rebuilding and visualization of three - dimensional nucleic acid structures." *Nucleic acids research* 31, no. 17 (2003): 5108-5121.
- [58]. Breen, Anthony P., and John A. Murphy. "Reactions of Oxyl Radicals with Dna." *Free Radical Biology and Medicine* 39, no. 10 (2005): 1269-1270.
- [59]. Pauling, Linus. "Evolution and the need for ascorbic acid." *Proceedings of the National Academy of Sciences* 67, no. 4 (1970): 1643-1648.
- [60]. Cameron, Ewan, Linus Pauling, and Brian Leibovitz. "Ascorbic acid and cancer: a review." *Cancer Research* 39, no. 3 (1979): 663-681.
- [61]. Fraga, Cesar G., Paul A. Motchnik, Mark K. Shigenaga, Harold J. Helbock, Robert A. Jacob, and Bruce N. Ames. "Ascorbic acid protects against endogenous oxidative DNA damage in human sperm." *Proceedings of the National Academy of Sciences* 88, no. 24 (1991): 11003-11006.
- [62]. Jacob, Stanley W., and C. Jack. *Dimethyl sulfoxide (DMSO) in trauma and disease*. CRC Press, 2015.
- [63]. Yu, Zhi-Wu, and Peter J. Quinn. "Dimethyl sulphoxide: a review of its applications in cell biology." *Bioscience reports* 14, no. 6 (1994): 259-281.

- [64]. Milligan, Jamie R., and John F. Ward. "Yield of single-strand breaks due to attack on DNA by scavenger-derived radicals." *Radiation research* 137, no. 3 (1994): 295-299.
- [65]. Hsiao, Ya-Yun, and Tzu-Hsiang Hung. "Computational Evaluation of Biological Effects of Dimethylsulphoxide for Radiotherapy." *Chung Shan Med. J.* 23, no. 2 (2012): 107-116.
- [66]. Runge, Roswitha, Liane Oehme, Jörg Kotzerke, and Robert Freudenberg. "The effect of dimethyl sulfoxide on the induction of DNA strand breaks in plasmid DNA and colony formation of PC Cl3 mammalian cells by alpha-, beta-, and auger electron emitters 223 Ra, 188 Re, and 99m Tc." *EJNMMI research* 6, no. 1 (2016): 48.
- [67]. Kashino, Genro, Yong Liu, Minoru Suzuki, Shin-ichiro Masunaga, Yuko Kinashi, Koji Ono, Keizo Tano, and Masami Watanabe. "An alternative mechanism for radioprotection by dimethyl sulfoxide; possible facilitation of DNA double-strand break repair." *Journal of radiation research* 51, no. 6 (2010): 733-740.
- [68]. Repine, John E., Oswald W. Pfenninger, David W. Talmage, Elaine M. Berger, and David E. Pettijohn. "Dimethyl sulfoxide prevents DNA nicking mediated by ionizing radiation or iron/hydrogen peroxide-generated hydroxyl radical." *Proceedings of the National Academy of Sciences* 78, no. 2 (1981): 1001-1003.
- [69]. Bishayee, Anupam, Dandamudi V. Rao, Lionel G. Bouchet, Wesley E. Bolch,

- and Roger W. Howell. "Protection by DMSO against cell death caused by intracellularly localized iodine-125, iodine-131 and polonium-210." *Radiation research* 153, no. 4 (2000): 416-427.
- [70]. Yokoya, A., N. Shikazono, K. Fujii, A. Urushibara, K. Akamatsu, and R. Watanabe. "DNA damage induced by the direct effect of radiation." *Radiation Physics and Chemistry* 77, no. 10-12 (2008): 1280-1285.
- [71]. Wiewior, Piotr P., Hideaki Shirota, and Edward W. Castner Jr. "Aqueous dimethyl sulfoxide solutions: Inter-and intra-molecular dynamics." *The Journal of chemical physics* 116, no. 11 (2002): 4643-4654.
- [72]. Anchordoguy, Thomas J., Christine A. Cecchini, John H. Crowe, and Lois M. Crowe. "Insights into the cryoprotective mechanism of dimethyl sulfoxide for phospholipid bilayers." *Cryobiology* 28, no. 5 (1991): 467-473.
- [73]. Cheng, Chi-Yuan, Jinsuk Song, Jolien Pas, Lenny HH Meijer, and Songi Han. "DMSO induces dehydration near lipid membrane surfaces." *Biophysical journal* 109, no. 2 (2015): 330-339.
- [74]. Iwatani, Misa, Kohta Ikegami, Yuliya Kremenska, Naka Hattori, Satoshi Tanaka, Shintaro Yagi, and Kunio Shiota. "Dimethyl sulfoxide has an impact on epigenetic profile in mouse embryoid body." *Stem Cells* 24, no. 11 (2006): 2549-2556.
- [75]. Holm, Frida, Susanne Ström, Jose Inzunza, Duncan Baker, Anne-Marie Strömberg, Björn Rozell, Anis Feki, Rosita Bergström, and Outi Hovatta. "An effective serum-and xeno-free chemically defined freezing procedure for human

- embryonic and induced pluripotent stem cells." *Human reproduction* 25, no. 5 (2010): 1271-1279.
- [76]. Rall, William F., and Gregory M. Fahy. "Ice-free cryopreservation of mouse embryos at- 196 C by vitrification." *Nature* 313, no. 6003 (1985): 573.
- [77]. Luzar, Alenka, and J. Stefan. "Dielectric behaviour of DMSO-water mixtures. A hydrogen-bonding model." *Journal of Molecular Liquids* 46 (1990): 221-238.
- [78]. Berz, David, Elise M. McCormack, Eric S. Winer, Gerald A. Colvin, and Peter J. Quesenberry. "Cryopreservation of hematopoietic stem cells." *American journal of hematology* 82, no. 6 (2007): 463-472.
- [79]. Rasmussen, D. H., and A. P. MacKenzie. "Phase diagram for the system water-dimethylsulphoxide." *Nature* 220, no. 5174 (1968): 1315.
- [80]. Lovelock, J. E., and M. W. H. Bishop. "Prevention of freezing damage to living cells by dimethyl sulphoxide." *Nature* 183, no. 4672 (1959): 1394.
- [81]. Schrader, Alex M., Chi-Yuan Cheng, Jacob N. Israelachvili, and Songi Han. "Communication: contrasting effects of glycerol and DMSO on lipid membrane surface hydration dynamics and forces." (2016): 041101.
- [82]. Kozikowski, Barbara A., Thomas M. Burt, Debra A. Tirey, Lisa E. Williams, Barbara R. Kuzmak, David T. Stanton, Kenneth L. Morand, and Sandra L. Nelson. "The effect of freeze/thaw cycles on the stability of compounds in DMSO." *Journal of biomolecular screening* 8, no. 2 (2003): 210-215.
- [83]. Yoshikawa, Yuko, Toshiaki Mori, Mari Suzuki, Tadayuki Imanaka, and Kenichi Yoshikawa. "Comparative study of kinetics on DNA double-strand break induced

- by photo-and gamma-irradiation: Protective effect of water-soluble flavonoids." *Chemical Physics Letters* 501, no. 1-3 (2010): 146-151.
- [84]. Ma, Yue, Naoki Ogawa, Yuko Yoshikawa, Toshiaki Mori, Tadayuki Imanaka, Yoshiaki Watanabe, and Kenichi Yoshikawa. "Protective effect of ascorbic acid against double-strand breaks in giant DNA: Marked differences among the damage induced by photo-irradiation, gamma-rays and ultrasound." *Chemical Physics Letters* 638 (2015): 205-209.
- [85]. Yoshikawa, Yuko, Kohji Hizume, Yoshiko Oda, Kunio Takeyasu, Sumiko Araki, and Kenichi Yoshikawa. "Protective effect of vitamin C against double-strand breaks in reconstituted chromatin visualized by single-molecule observation." *Biophysical journal* 90, no. 3 (2006): 993-999.
- [86]. Yoshikawa, Yuko, Toshiaki Mori, Nobuyuki Magome, Kumiko Hibino, and Kenichi Yoshikawa. "DNA compaction plays a key role in radioprotection against double-strand breaks as revealed by single-molecule observation." *Chemical Physics Letters* 456, no. 1-3 (2008): 80-83.
- [87]. Meng, X. C., C. Stanton, G. F. Fitzgerald, C. Daly, and R. P. Ross. "Anhydrobiotics: The challenges of drying probiotic cultures." *Food Chemistry* 106, no. 4 (2008): 1406-1416.
- [88]. Pegg, David E. "Principles of cryopreservation." In *Cryopreservation and freeze-drying protocols*, pp. 39-57. Humana Press, 2007.
- [89]. Costanzo, J. P., RICHARD E. Lee Jr, and MICHAEL F. Wright. "Glucose loading prevents freezing injury in rapidly cooled wood frogs." *American*

- Journal of Physiology-Regulatory, Integrative and Comparative Physiology* 261, no. 6 (1991): R1549-R1553.
- [90]. Mazur, Peter. "Cryobiology: the freezing of biological systems." *Science* 168, no. 3934 (1970): 939-949.
- [91]. Noda, Masami, Yue Ma, Yuko Yoshikawa, Tadayuki Imanaka, Toshiaki Mori, Masakazu Furuta, Tatsuaki Tsuruyama, and Kenichi Yoshikawa. "A single-molecule assessment of the protective effect of DMSO against DNA double-strand breaks induced by photo-and γ -ray-irradiation, and freezing." *Scientific reports* 7, no. 1 (2017): 8557.
- [92]. Baase, Walter A., and W. Curtis Johnson Jr. "Circular dichroism and DNA secondary structure." *Nucleic acids research* 6.2 (1979): 797-814.
- [93]. Zeugin, Jil A., and James L. Hartley. "Ethanol precipitation of DNA." *Focus* 7.4 (1985): 1-2.
- [94]. Gaillard, Claire, and Fran ois Strauss. "Ethanol precipitation of DNA with linear polyacrylamide as carrier." *Nucleic Acids Research* 18.2 (1990): 378.
- [95]. Wilson, Kate. "Preparation of genomic DNA from bacteria." *Current protocols in molecular biology* (1987): 2-4.
- [96]. Raeder, U., and P. Broda. "Rapid preparation of DNA from filamentous fungi." *Letters in Applied Microbiology* 1.1 (1985): 17-20.
- [97]. Paterson, Andrew H., Curt L. Brubaker, and Jonathan F. Wendel. "A rapid method for extraction of cotton (*Gossypium* spp.) genomic DNA suitable for RFLP or PCR analysis." *Plant Molecular Biology Reporter* 11.2 (1993):

122-127.

- [98]. Wilson, Kate. "Preparation of genomic DNA from bacteria." *Current protocols in molecular biology* (1987): 2-4.
- [99]. Gaillard, Claire, and Fran ois Strauss. "Ethanol precipitation of DNA with linear polyacrylamide as carrier." *Nucleic Acids Research* 18.2 (1990): 378.
- [100]. Paithankar, K. R., and K. S. Prasad. "Precipitation of DNA by polyethylene glycol and ethanol." *Nucleic acids research* 19.6 (1991): 1346.
- [101]. Michaels, S. D., M. C. John, and R. M. Amasino. "Removal of polysaccharides from plant DNA by ethanol precipitation." *Biotechniques* 17.2 (1994): 274-276.
- [102]. Crouse, Joseph, and Douglas Amorese. "Ethanol precipitation: ammonium acetate as an alternative to sodium acetate." *Focus* 9.2 (1987): 3-5.
- [103]. Wallace, Donald M. "[5] Precipitation of nucleic acids." *Methods in enzymology*. Vol. 152. Academic Press, 1987. 41-48.
- [104]. Horn, Nancy A., et al. "Cancer gene therapy using plasmid DNA: purification of DNA for human clinical trials." *Human Gene Therapy* 6.5 (1995): 565-573.
- [105]. Piškur, Jure, and Allan Rupprecht. "Aggregated DNA in ethanol solution." *FEBS letters* 375.3 (1995): 174-178.
- [106]. Allen, John Michael, et al. "Carboxyalkyl cellulose esters." U.S. Patent No. 5,668,273. 16 Sep. 1997.
- [107]. Posey-Dowty, Jessica Dee, et al. "Carboxyalkyl cellulose esters for use in aqueous pigment dispersions." U.S. Patent No. 5,994,530. 30 Nov. 1999.
- [108]. Nishi, Nobuyuki, et al. "Hydrogen-Bonding Cluster Formation and

- Hydrophobic Solute Association in Aqueous-Solution of Ethanol." *Journal of Physical Chemistry* 99.1 (1995): 462-468.
- [109]. Matsumoto, Masaki, et al. "Structure of clusters in ethanol–water binary solutions studied by mass spectrometry and X-ray diffraction." *Bulletin of the Chemical Society of Japan* 68.7 (1995): 1775-1783.
- [110]. Dixit, S., et al. "Molecular segregation observed in a concentrated alcohol–water solution." *Nature* 416.6883 (2002): 829-832.
- [111]. Turner, J., and A. K. Soper. "The effect of apolar solutes on water structure: Alcohols and tetraalkylammonium ions." *The Journal of chemical physics* 101.7 (1994): 6116-6125.
- [112]. Koga, Yoshikata. "Fluctuations in aqueous methanol, ethanol, and propan-1-ol: amplitude and wavelength of fluctuation." *Canadian Journal of Chemistry* 77.12 (1999): 2039-2045.
- [113]. Großmann, Georg H., and Klaus H. Ebert. "Formation of Clusters in 1-Propanol/Water-Mixtures." *Berichte der Bunsengesellschaft für physikalische Chemie* 85.11 (1981): 1026-1029.

Curriculum Vitae

Ma Yue

DATE of BIRTH: September 10th, 1992

PLACE of BIRTH: Ningxia, China

EDUCATION

2015 Doshisha University (Kyoto, Japan)

M.E. Life and Medical Sciences

2013 Sun Yat-sen University (Guangdong, China)

B.S. Physics

PROFESSIONAL MEMBERSHIPS

The Biophysical Society of Japan

Japan Society of Applied Physics

May 2018

List of Publication

1. Yue Ma, Naoki Ogawa, Yuko Yoshikawa, Toshiaki Mori, Tadayuki Imanaka, Yoshiaki Watanabe, and Kenichi Yoshikawa. "Protective effect of ascorbic acid against double-strand breaks in giant DNA: Marked differences among the damage induced by photo-irradiation, gamma-rays and ultrasound." *Chemical Physics Letters* 638 (2015): 205-209.

2. Masami Noda, Yue Ma, Yuko Yoshikawa, Tadayuki Imanaka, Toshiaki Mori, Masakazu Furuta, Tatsuaki Tsuruyama, and Kenichi Yoshikawa. "A single-molecule assessment of the protective effect of DMSO against DNA double-strand breaks induced by photo-and γ -ray-irradiation, and freezing." *Scientific reports* 7, no. 1 (2017): 8557.

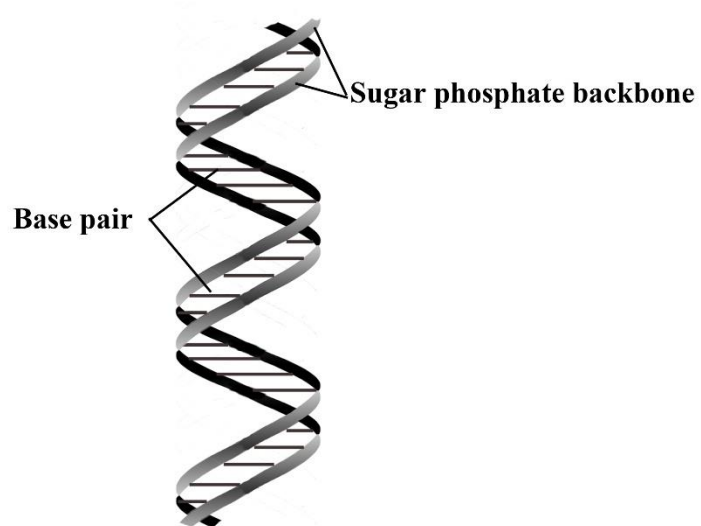


Figure 1.1 Schematic illustrations of a DNA double helix

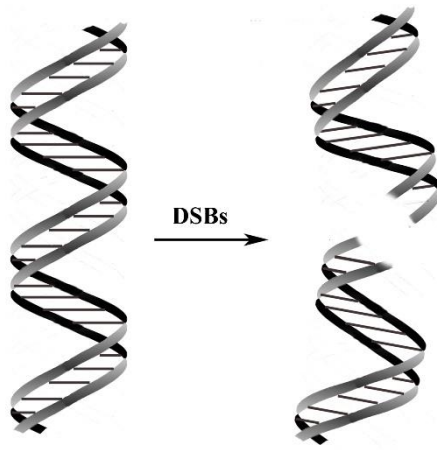


Figure 1.2 Schematic illustrations of a double-strand breaks (DSBs).

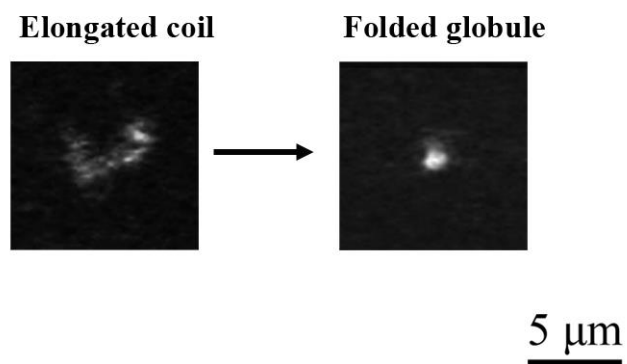


Figure 1.3 A representative fluorescence image of DNA transition from elongated coil to compacted globule states (λ DNA)

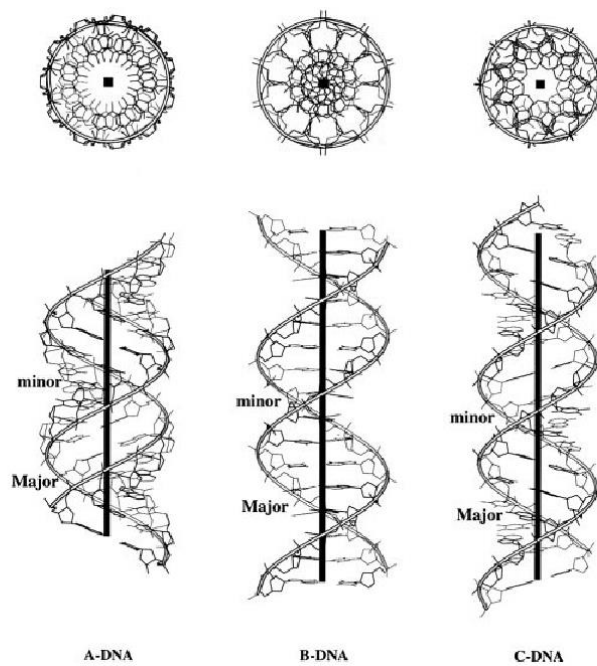


Figure 1.4 Schematic of A-form, B-form and C-form DNA[57]

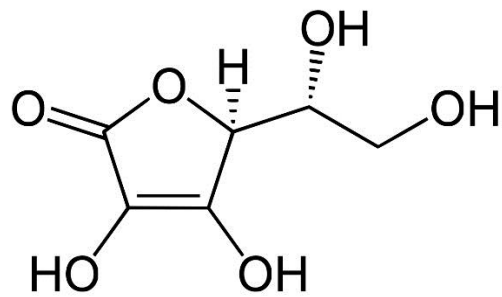


Figure 2.1 the chemical formula of ascorbic acid

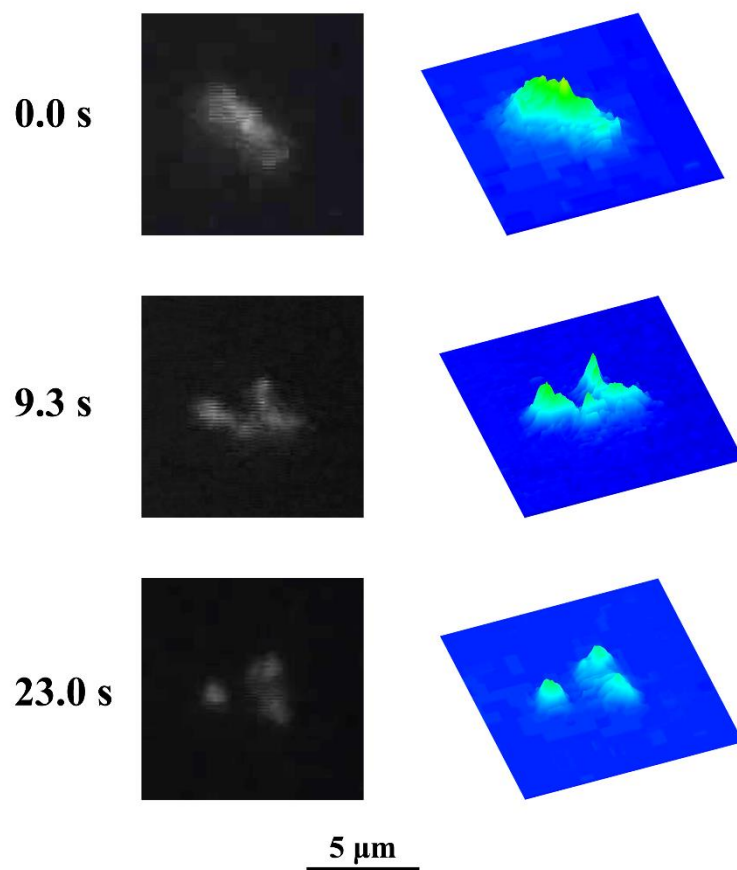


Figure 2.2 Example of the real-time observation of double-strand breaks.

Fluorescence microscopic images on a single T4 DNA molecule under photo-irradiation (left) and the corresponding quasi-three-dimensional profiles of the fluorescence-intensity distribution (right). (Fluorescent dye YOYO-1: 0.05 μM , Ascorbic acid: 1.0 mM)

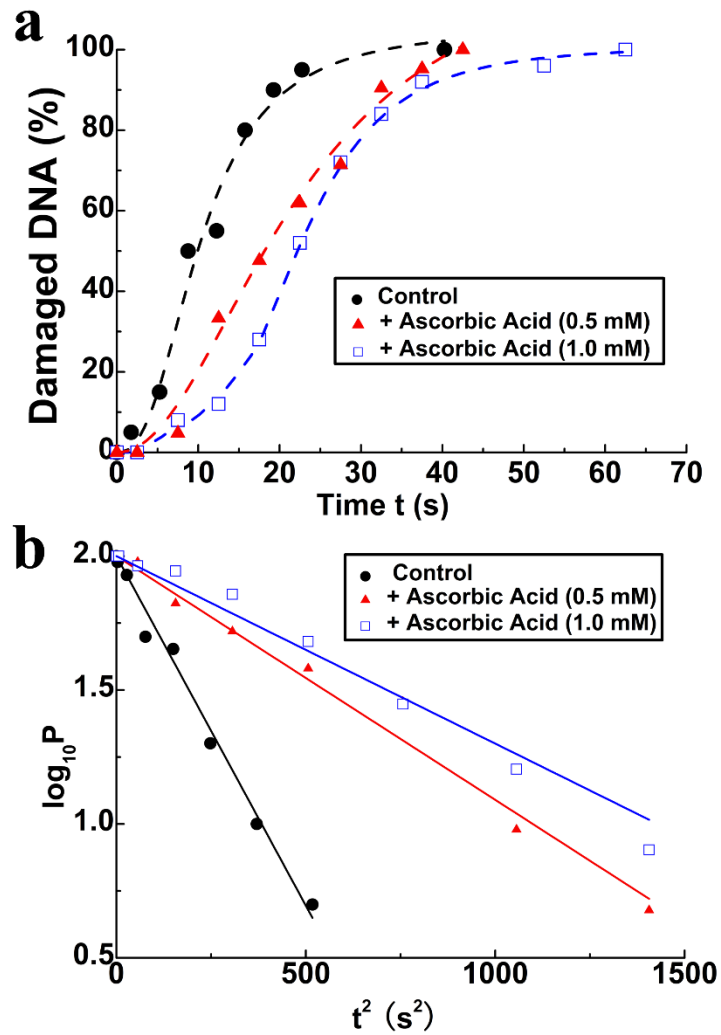


Figure 2.3 Photo-induced DSBs. (a) Time-dependence of the percentage of damaged DNA molecules. (b) Relationship between t^2 and $\log_{10}P$. (P is the percentage of surviving DNA molecules under photo-irradiation, which was calculated as $[100\% - (\text{percentage of damaged DNA})]$)

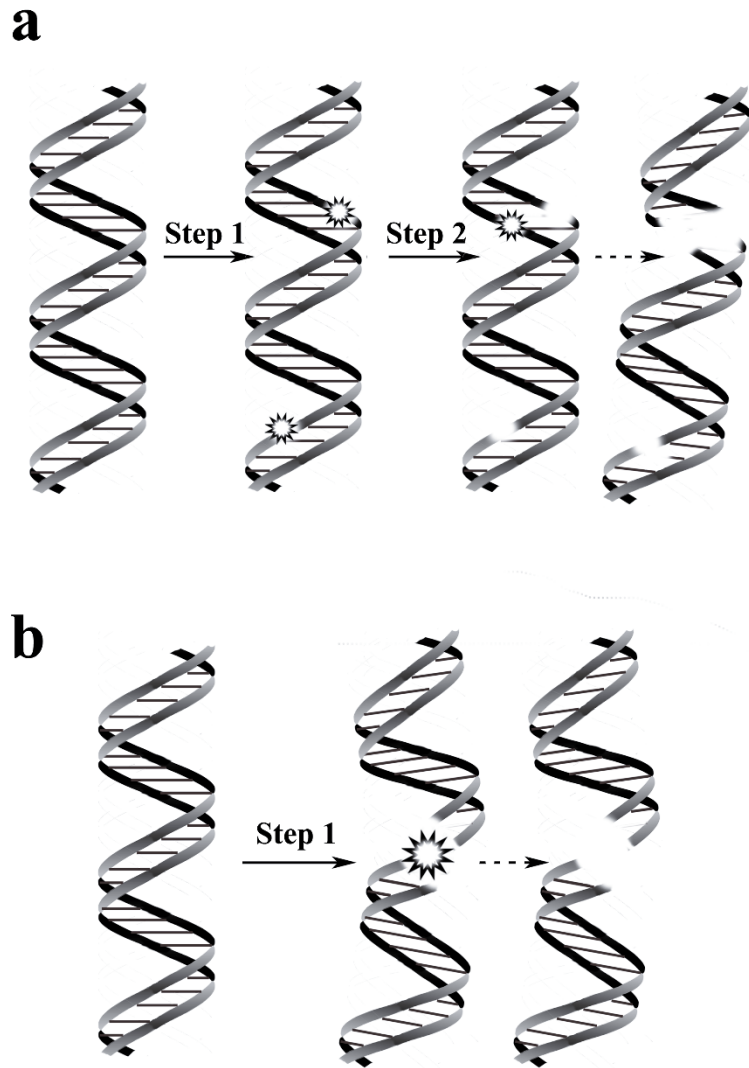


Figure 2.4 Schematic illustrations of a double-strand break.

(a) Two-step mechanism. (b) One-step mechanism.

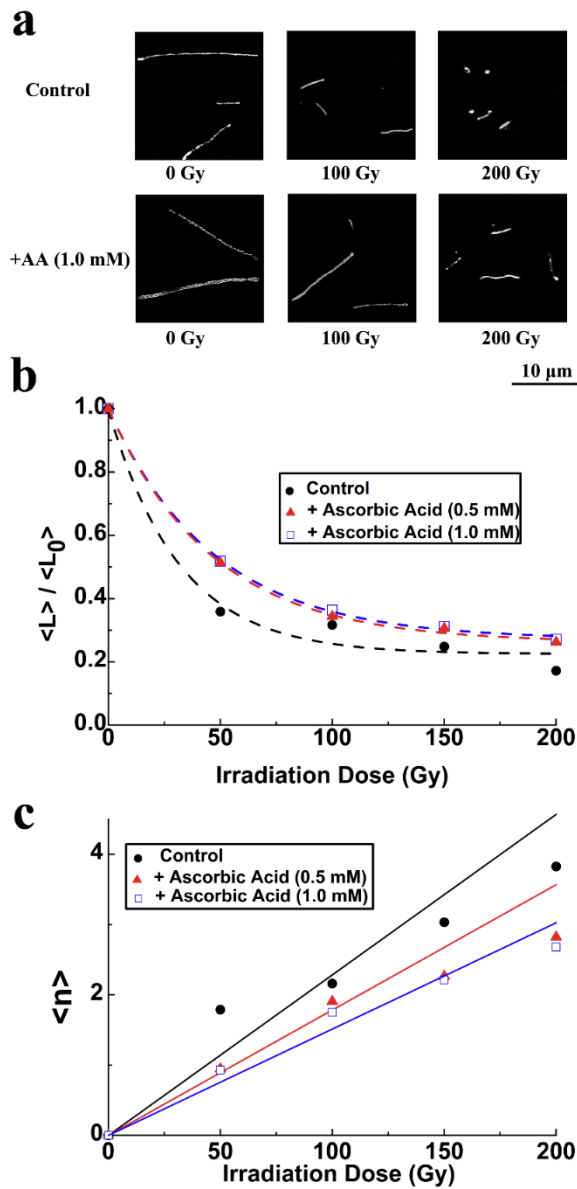


Figure 2.5 γ -ray-induced DSBs. (a) Fluorescence microscopic images of DNA molecules fixed on a glass surface after irradiation with different doses of γ -rays. (b) Average lengths of DNA, $\langle L \rangle$, vs. the irradiation dose of γ -rays. (c) Number of DSBs per DNA molecule, $\langle n \rangle$, vs. the irradiation dose of γ -rays.

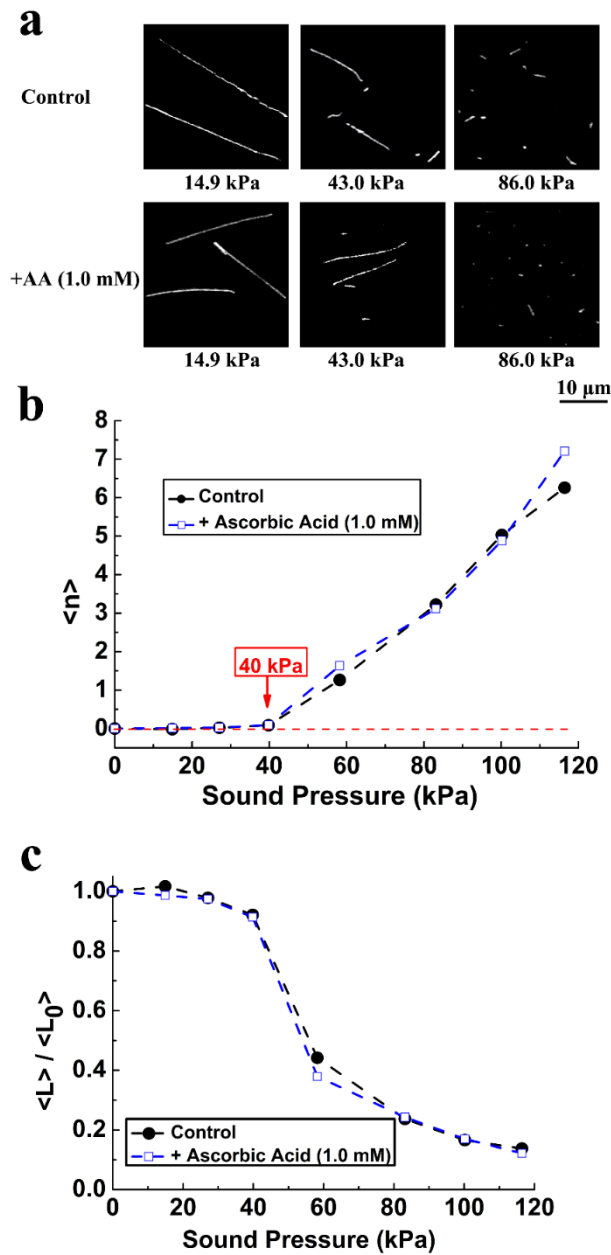


Figure 2.6 Ultrasound-induced DSBs. (a) Fluorescence microscopic images of DNA molecules fixed on a glass surface after exposure to ultrasound at different sound pressures. (b) Average lengths of DNA, $\langle L \rangle$, vs. the sound pressure of ultrasound. (c) Number of DNA double-strand breaks per molecule, $\langle n \rangle$, vs. the sound pressure of ultrasound.

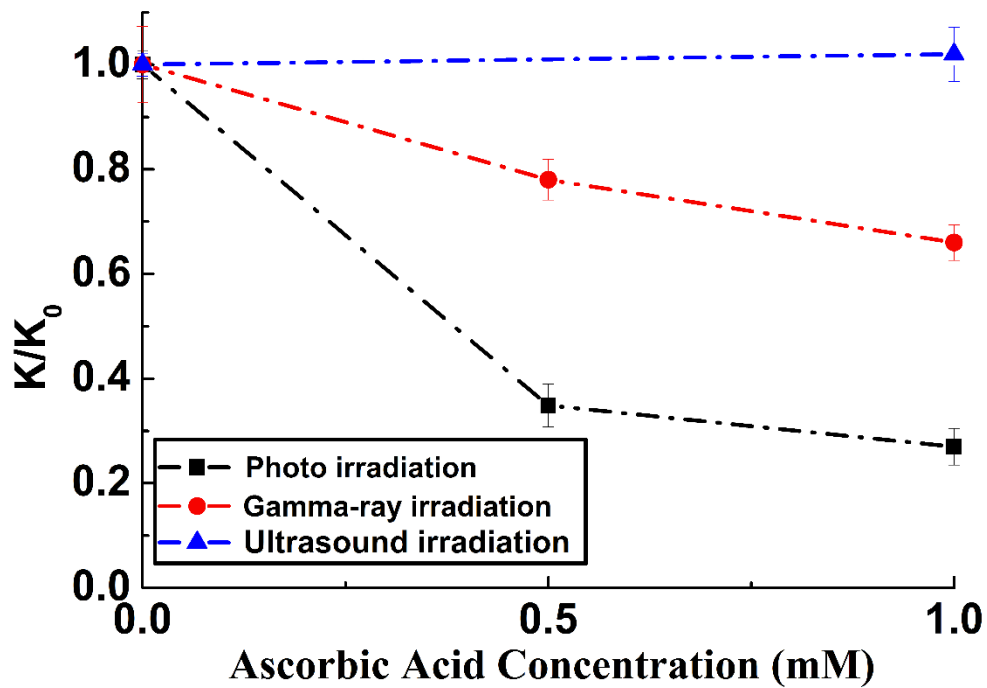


Figure 2.7 Difference in the protective effect of AA. Vertical axis is the relative kinetic constant K/K_0 on the reaction to cause DSBs at different concentrations of ascorbic acid, where K_0 is the rate constant in the absence of AA. (For ultrasound-induced DNA damage, the kinetic constants are adapted from the threshold sound pressure, whereas the data are essentially the same for the kinetic parameters provided from the slopes, as shown in Fig.5c.)

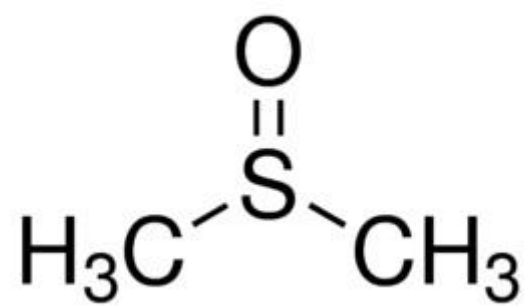


Figure 3.1 the chemical formula of DMSO

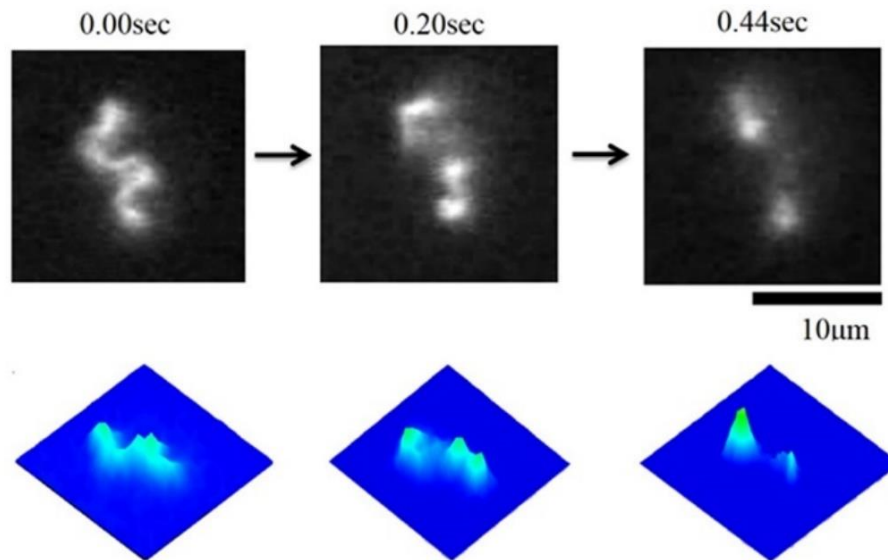


Figure 3.2 Example of the real-time observation of DSB caused by photo-irradiation-induced ROS. Fluorescence microscopic images of a single T4 DNA molecule under photo-irradiation (upper), and the corresponding quasi-three-dimensional profiles of the fluorescence intensity distribution (bottom). (Fluorescence dye: 0.05 μM YOYO-1 in the absence of DMSO).

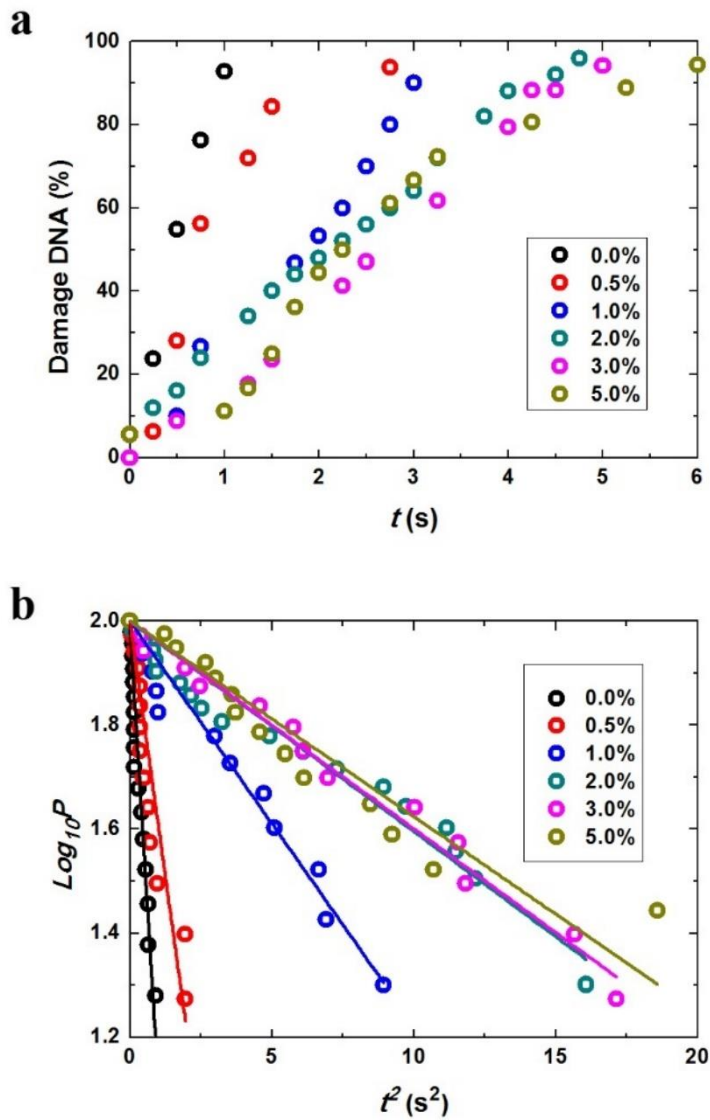


Figure 3.3 Photo-induced DSBs. (a) Time-dependence of the percentage of damaged DNA molecules at different DMSO concentrations. (b) The relationship between t^2 and $\log_{10}P$, where P is the percentage of surviving DNA molecules, which was calculated as $[100\% - (\text{percentage of damaged DNA})]$. (The kinetic constants, K_v 's (s⁻²), are evaluated from the slopes of Figure 2b.) (For DMSO's concentration on 2% and 3%, fitting lines are coincided since their slopes are very close.)

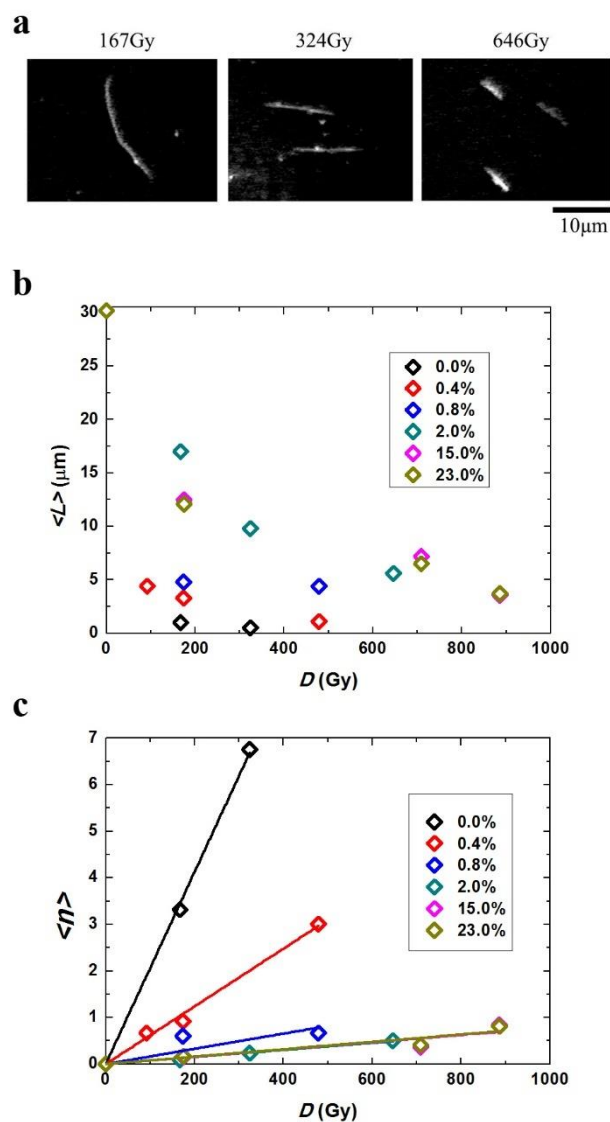


Figure 3.4 DSBs induced by γ -ray. (a) Fluorescence microscopic images of DNA molecules fixed on a glass surface after irradiation with different doses of γ -ray. (b) Average DNA lengths, $\langle L \rangle$, vs. the irradiation dose of γ -rays. (c) Number of DSBs per 10 kbp, $\langle n \rangle$, vs. the irradiation dose of γ -rays. (The kinetic constants, $K\gamma$'s (Gy), are evaluated from the slopes of Figure 3c.) (As DMSO's concentration beyond 2%, fitting lines are coincided since their slopes are very close.)

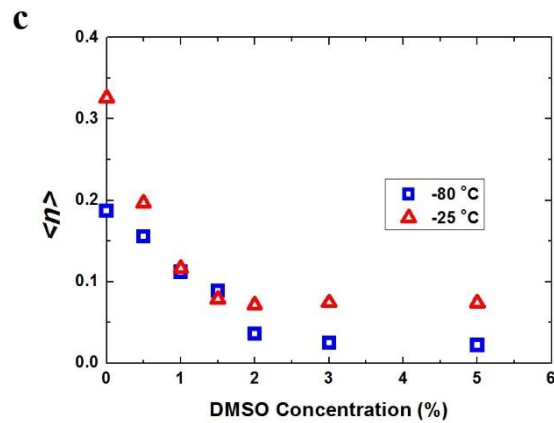
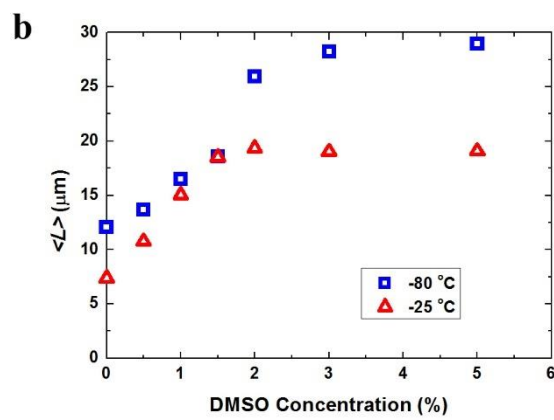
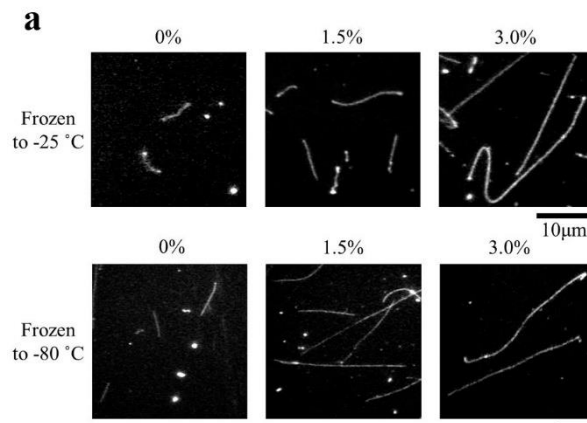


Figure 3.5 Freezing-induced DSBs. (a) Single DNA image after freeze/thawing to $-25\text{ }^{\circ}\text{C}$ (upper: slow frozen) and $-80\text{ }^{\circ}\text{C}$ (lower: quick frozen). (b) Average lengths of DNA, $\langle L \rangle$, vs. the concentration of DMSO. (c) The number of DSBs per 10 kbp, $\langle n_f \rangle$, vs. the concentration of DMSO.

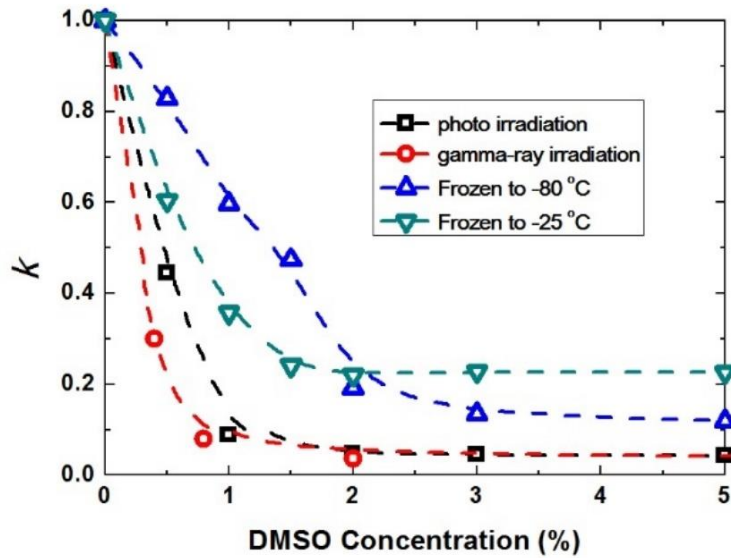


Figure 3.6 Difference in the protective effect of DMSO. Vertical axis is the relative kinetic constant $k = K/K_0$ for the generation of DSBs at different concentrations of DMSO, where K_0 is the rate constant in the absence of DMSO. With respect to freezing, quickfreezing is to $-80\text{ }^\circ\text{C}$, and slow freezing is to $-25\text{ }^\circ\text{C}$.

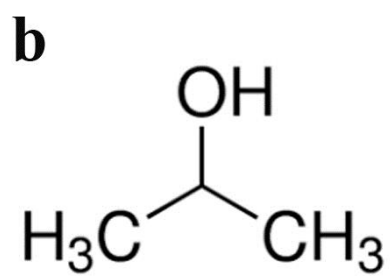
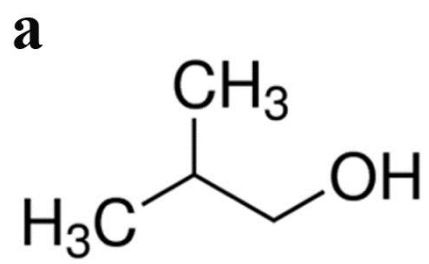


Figure 4.1 the chemical formula of (a)1-propanol and (b) 2-propanol

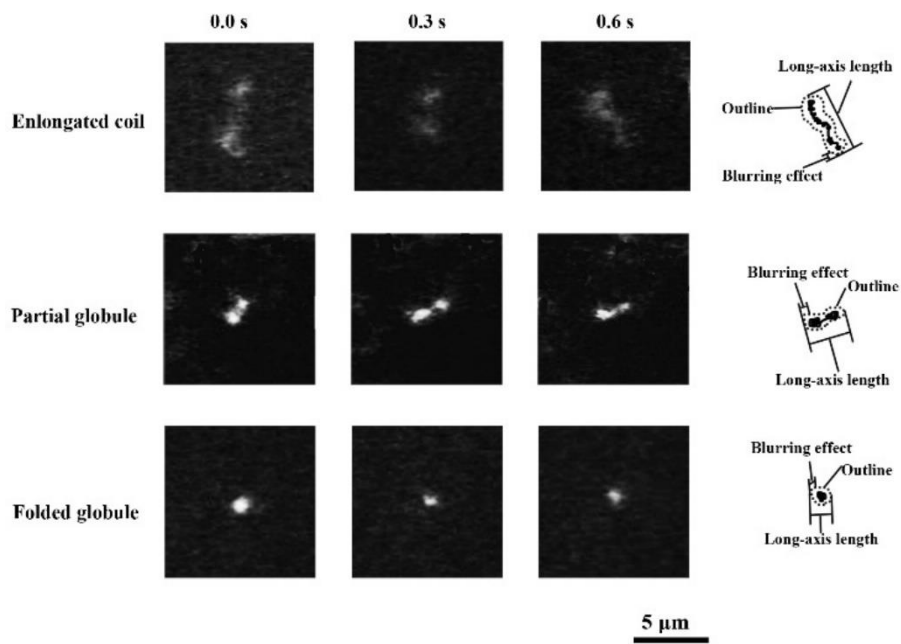


Figure 4.2 Fluorescence images of representative styles of DNA molecules in solutions [propanol concentration of samples from up to below: 0%, 50%, 80% (v/v) (1-propanol)]

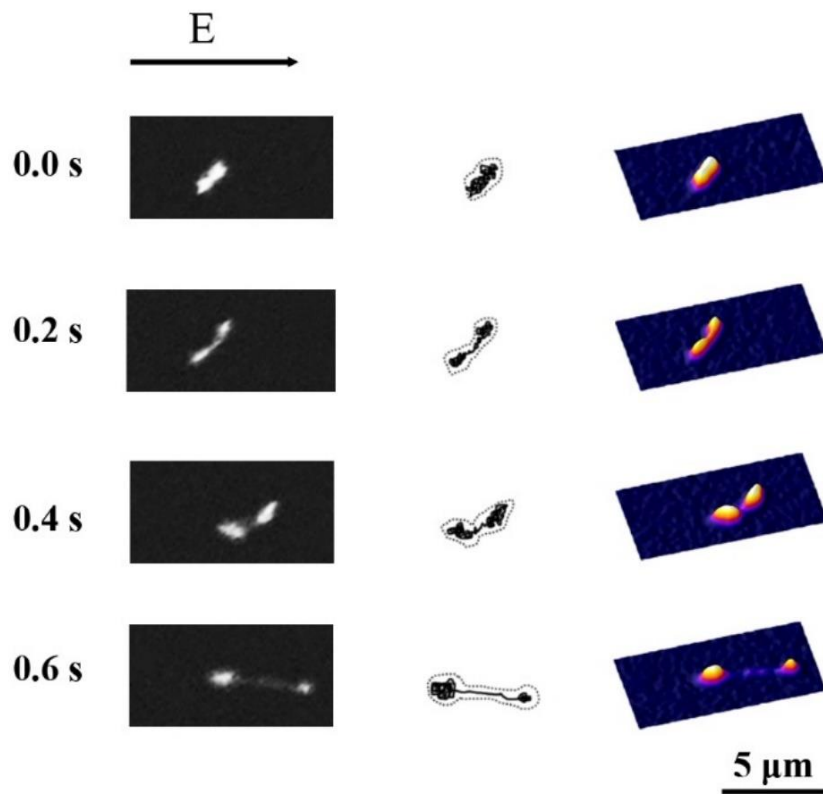


Figure 4.3 After applied an electric field around $\sim 10 \text{ V/cm}$ to the DNA samples, the coiled and globular states separated

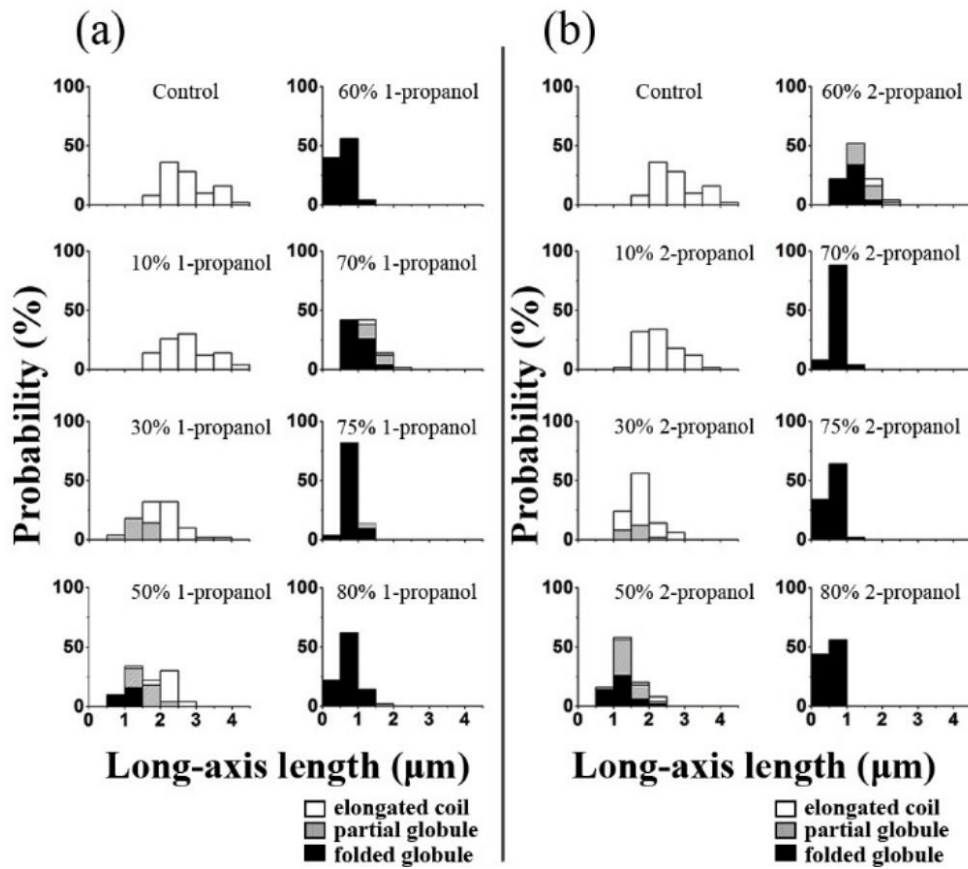


Figure 4.4 Distribution of long-axis length of DNA molecules in propanol solutions.

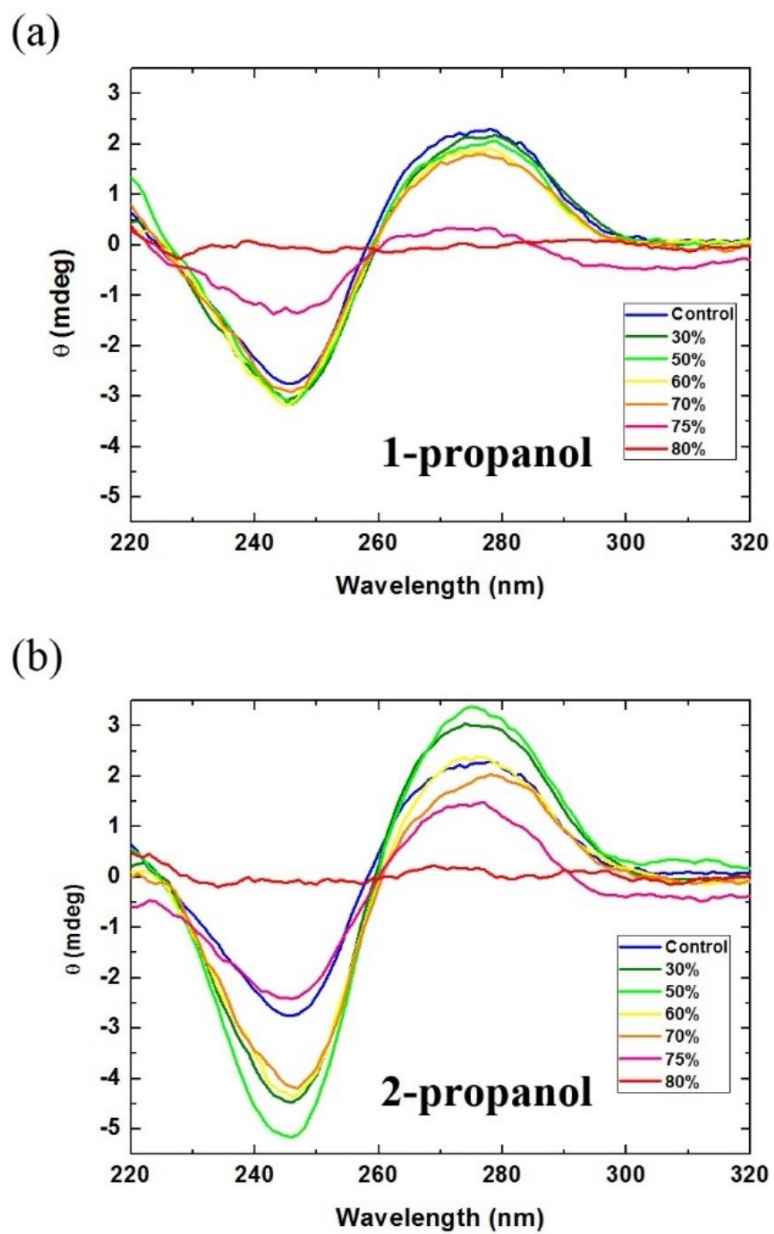


Figure 4.5 CD spectra of DNA (λ -DNA, 30 μ M in nucleotide units) at different propanol solutions.

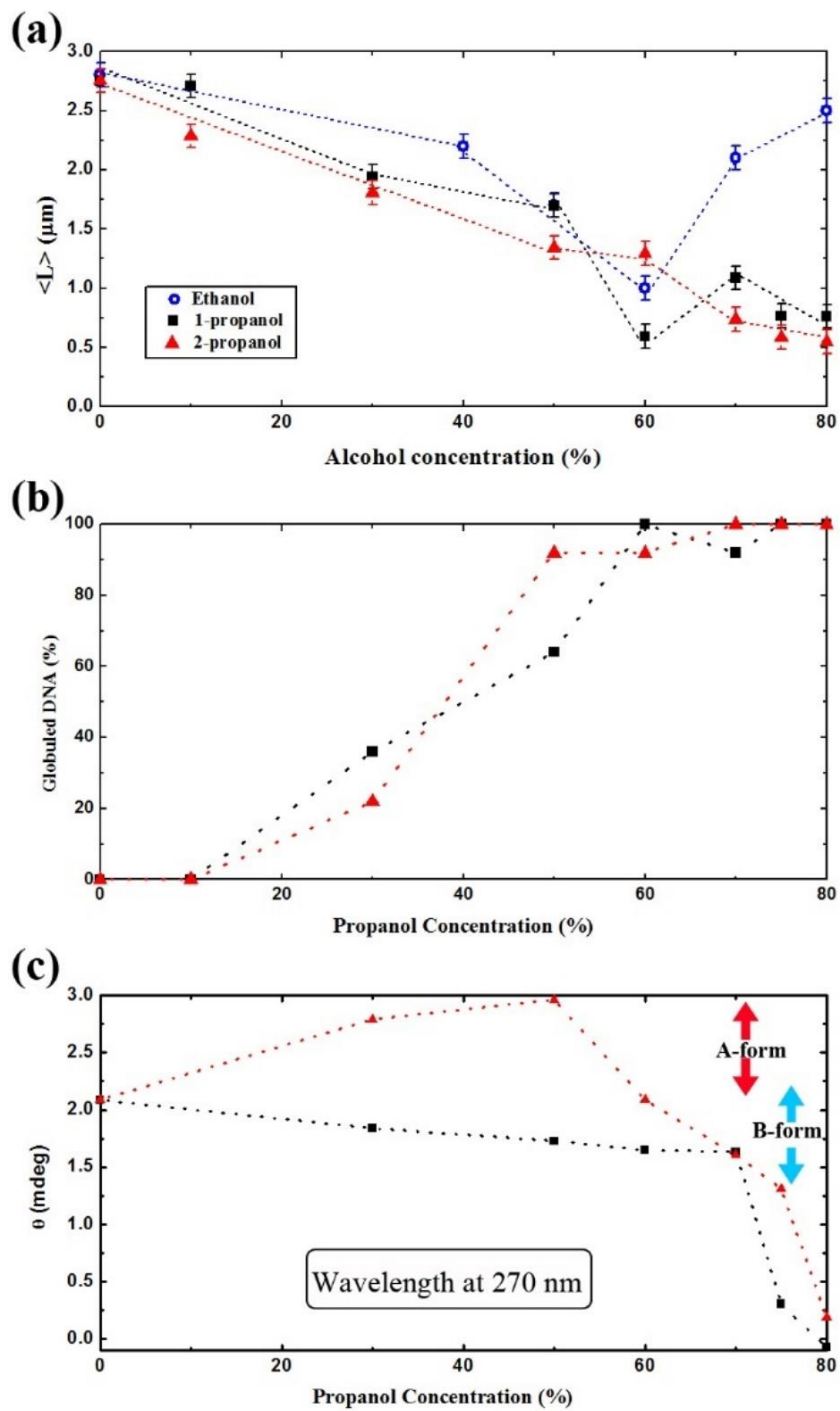


Figure 4.6 (a) The average long-axis length of DNA molecules at different alcohol solutions; (b) The globular rate of DNA samples at different propanol solutions; (c)

Degrees of ellipticity (θ) of CD spectra of DNA samples at 270 nm